

Potent 3-hydroxy-2-pyridine aldoxime reactivators of organophosphate-inhibited cholinesterases with predicted blood-brain barrier penetration

Tamara Zorbaz,^[a] Anissa Braïki,^[b] Nikola Maraković,^[a] Julien Renou,^[b] Eugenio de la Mora,^[c] Nikolina Maček Hrvat,^[a] Maja Katalinić,^[a] Israel Silman,^[d] Joel L. Sussman,^[e] Guillaume Mercey,^[b] Catherine Gomez,^[b] Romain Mougeot,^[b] Belén Pérez,^[f] Rachid Baati,^[g] Florian Nachon,^[h] Martin Weik,^[c] Ludovic Jean,^{*[b]} Zrinka Kovarik^{†[a]} and Pierre-Yves Renard^{*[b]}

Abstract: A new series of 3-hydroxy-2-pyridine aldoxime compounds were designed, synthesized and tested *in vitro*, *in silico* and *ex vivo* as reactivators of human acetylcholinesterase (hAChE) and butyrylcholinesterase (hBChE) inhibited by organophosphates (OPs) (e.g., VX, sarin, cyclosarin, tabun and paraoxon). The reactivation rates of three oximes (**16**, **17**, **18**) were greater than those of 2-PAM, and comparable to HI-6, two pyridinium aldoximes currently used by the armies of several countries worldwide. The important interactions for a productive orientation of the oxime group within the OP-inhibited enzyme were clarified by molecular modelling studies and by the resolution of the crystal structure of the complex of **17** with *Torpedo californica* AChE. The prediction of blood-brain barrier penetration was carried out for oximes **15–18** based on their physicochemical properties and *in vitro* brain membrane permeation

assay. Among the evaluated compounds, two morpholine-3-hydroxy pyridine aldoxime conjugates showed to be promising reactivators of OP-inhibited cholinesterases. Moreover, *ex vivo* efficient reactivation of phosphorylated native cholinesterases by selected oximes enabled significant hydrolysis of VX, sarin, paraoxon and cyclosarin in whole human blood implying a scavenging potential of the oximes.

Introduction

Organophosphorus compounds (OPs) were originally developed as pesticides, but due to their non-selective species toxicity, they were also used as nerve agents (**Figure 1**). Annually, pesticide intoxication causes 200,000 fatalities worldwide,^[1] while nerve agents have been used in several terrorist attacks against civilians (e.g., Matsumoto, Japan, 1994; Tokyo subway, 1995), and most recently during the civil war in Syria^[2] and the assassination with VX at the Malaysian airport. Since September 11, 2001 research on the mechanisms of action of OPs, and pretreatments and treatments that prevent or reverse their severe biological effects has intensified.

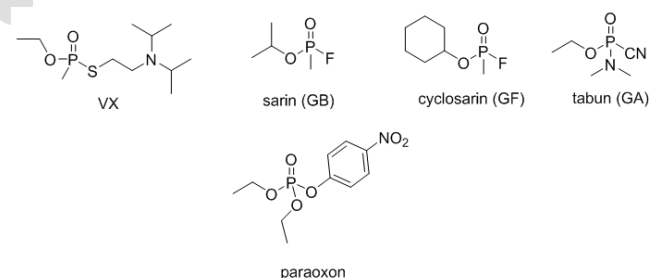


Figure 1 Nerve agents (top line) and pesticide (lower line) used in this study

The acute toxicity of OPs is due to the irreversible inhibition of acetylcholinesterase (AChE, EC 3.1.1.7). This key enzyme regulates the cholinergic transmission in the peripheral and central nervous systems by rapid hydrolysis of the neurotransmitter acetylcholine (ACh). AChE inhibition leads to accumulation of ACh at neuronal synapses and neuromuscular junctions, resulting in paralysis, seizures, respiratory arrest, and/or death.^[3] In addition, long-term central nervous system impairments (i.e., cognitive and behavioural deficits) have been observed in survivors of OP poisoning due to neurotoxic

- [a] T. Zorbaz, Dr. N. Maraković, Dr. N. Maček Hrvat, Dr. M. Katalinić, Dr Z. Kovarik*
Institute for Medical Research and Occupational Health
Ksaverska cesta 2, HR-10000 Zagreb, Croatia
E-mail: zkovarik@imi.hr
- [b] A. Braïki, Dr. J. Renou, G. Mercey, C. Gomez, R. Mougeot, Prof. L. Jean*, Prof. P.-Y. Renard*
COBRA (UMR 6014), INSA Rouen, CNRS, Normandie Univ, UNIROUEN, 76000 Rouen, France
E-mail: ludovic.jean@univ-rouen.fr; pierre-yves.renard@univ-rouen.fr
- [c] Dr. E. de la Mora, Dr. M. Weik
Univ Grenoble Alpes, CEA, CNRS, IBS, 38000 Grenoble, France
- [d] Prof. I. Silman
Department of Neurobiology, Weizmann Institute of Science
6100 Rehovot, Israel
- [e] Prof. J. Sussman
Department of Structural Biology, Weizmann Institute of Science
76100 Rehovot, Israel
- [f] Prof. B. Perez
Departament de Farmacologia, de Terapèutica i de Toxicologia
Universitat Autònoma de Barcelona
08193, Bellaterra, Barcelona, Spain
- [g] Prof Rachid Baati
Institut de Chimie et Procédés pour l'Energie, l'Environnement et la Santé (ICPEES), ECPM, UMR 7515 CNRS - Université de Strasbourg, 25 rue Becquerel, Strasbourg 67087 Cedex 02, France
- [h] Dr. F. Nachon
Département de Toxicologie et Risques Chimiques
Institut de Recherche Biomédicale des Armées
91220 Brétigny-sur-Orge, France

T.Z. and A.B. contributed equally to this study.

Supporting information for this article is given via a link at the end of the document

mechanisms that lead to neuronal damage in specific brain regions.^[4] Butyrylcholinesterase (BChE, EC 3.1.1.8) also hydrolyses ACh effectively. BChE's physiological role is not yet understood, but it protects AChE from OPs and may be indirectly involved in the regulation of the cholinergic system.^[5] Emergency treatment of OP poisoning involves a rapid administration of a cocktail composed of an antimuscarinic agent (e.g., atropine), a pyridinium oxime as an AChE reactivator (standard oximes employed include 2-PAM, obidoxime and HI-6, and; **Figure 2**) and an anticonvulsant drug (e.g., diazepam).^[6]

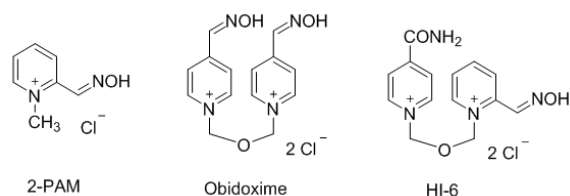


Figure 2 Chemical structures of standard pyridinium oximes in use

An oxime reactivates the OP-inhibited enzyme by nucleophilic displacement of the OP moiety bound to the catalytic serine of the cholinesterase (ChE) active site.^[7] Although both AChE and BChE share the same mechanism of hydrolysis of substrates that includes the formation of a Michaelis-type complex, acylation of the catalytic serine, and spontaneous deacylation with a water molecule, the difference in amino acid residues composition in the active site domains, such as acyl pocket, choline binding site and peripheral site, directs the specificities and sensitivities of AChE and BChE to a wide range of ligands and inhibitors.^[8] It is worth mentioning that the phosphorylation of the enzymes by OPs is analogous to the mechanism of hydrolysis (i.e., OPs are structural analogues of substrate transition state in hydrolysis)^[9] and results in a structurally different phosphorylated enzyme conjugate. Therefore, no single oxime, reported in the literature, is equally efficient against a variety of OPs and potent for both AChE and BChE.

Numerous mono- and bispyridinium oximes with a quaternary nitrogen atom, analogous to the standard oximes (**Figure 2**), have been synthesized and tested so far.^[10] However, due to their permanent positive charge, they do not cross the blood-brain barrier (BBB) efficiently^[11] and hence do not reactivate brain AChE.^[12] Therefore, in recent years, several research teams have focused their efforts on developing a new generation of AChE reactivators including uncharged molecules with protonatable groups.^[13]

In this context we described the synthesis of new uncharged 3-hydroxy-2-pyridine aldoxime reactivators connected *via* an aliphatic linker (with four to five methylene groups) to simple protonatable tertiary amines (morpholine, piperidine) that can be fused with dimethoxybenzene (dimethoxy-tetrahydroisoquinoline) and substituted with *N,N*-dimethylaniline (1-(4-*N,N*-dimethylamino phenyl)-1,2,3,4-tetrahydroisoquinoline) (**Figure 3**). These substituents were chosen to improve the binding affinity facilitating cation- π or π - π stacking interactions with residues in the peripheral site of the enzyme. In addition, such oximes are more prone to passive transport across the membranes because they are ampholytes with a tertiary amine

group with a $pK_a \sim 8$, having also a fraction of non-ionized species.^[13n, 14] Indeed, the neutral species can be expected to cross the blood-brain barrier delivering the reactivator into the brain, and upon establishing the pH-dependent ionization equilibrium in the CNS, the ionized form would have the best chance of productive interaction with the OP-inhibited enzyme, because the protonated amine form is efficiently attracted to the electron rich active centre environment of the inhibited AChE.^[15] The novel compounds were thoroughly characterized in terms of their inhibitory effect on human AChE (hAChE) and BChE (hBChE), and tested against VX-, tabun-, sarin-, cyclosarin- and paraoxon-inhibited hAChE and hBChE. The crystallographic structure of TcAChE in complex with oxime **17**, together with molecular docking studies of several oximes within OP-inhibited cholinesterases revealed the favourable orientation and interactions of oximes within the enzymatic active site gorge. Furthermore, the potency of these oximes to cross the BBB was predicted by *in silico* studies based on their physicochemical properties and the *in vitro* parallel artificial membrane permeation assay (PAMPA). In addition to the potent *in vitro* reactivation, a pseudo-catalytic scavenging system (i.e., degradation of an OP by an oxime together with native cholinesterases) was investigated *ex vivo* as a potential approach to treatment of OP poisoning as previously reported.^[16]

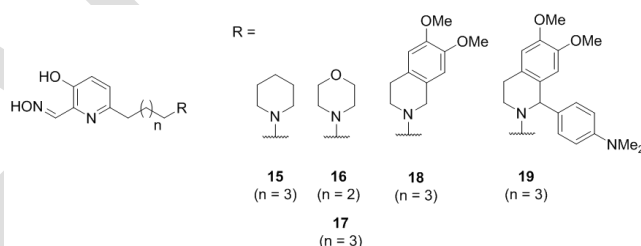
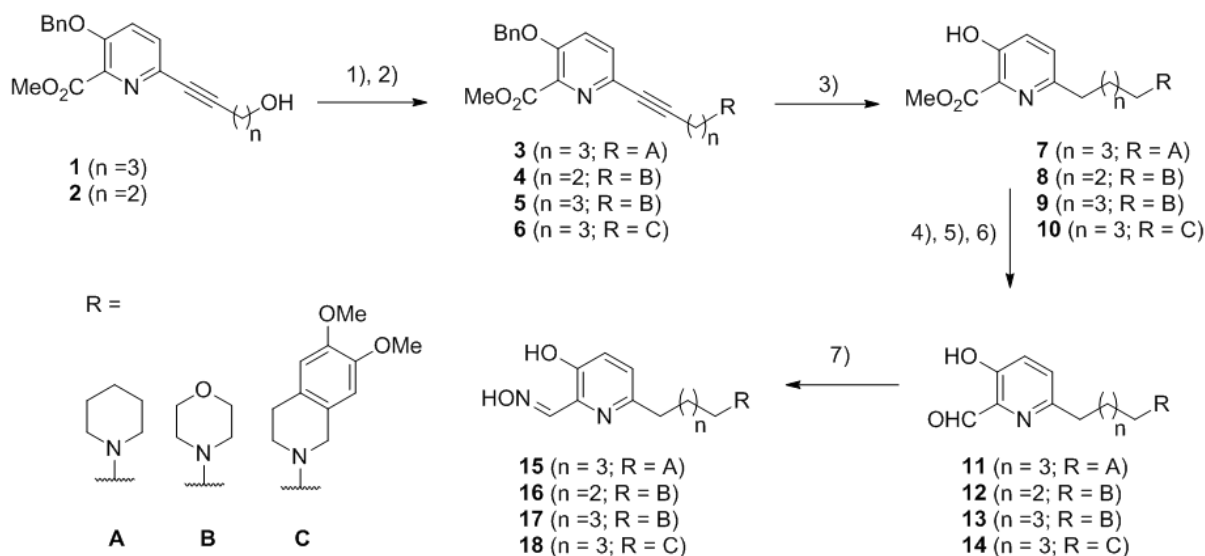


Figure 3. Structure of 3-hydroxy-2-pyridine aldoxime reactivators

Results

Oxime synthesis. The synthesis of oximes **15–19** followed the strategy for the preparation of uncharged reactivators (**Scheme 1**) developed previously (see supporting information).^{[13], [k]} From compounds **1** or **2** the first step consisted in forming the corresponding mesylates followed by a nucleophilic substitution with the secondary amine **A–C**. Compounds **3–6** were prepared at a yield of 36–72% (two steps). Then concomitant reduction of the alkyne and deprotection of the phenol function was carried out using Pearlman's catalyst under a H_2 atmosphere to obtain compounds **7–10** with a 53–99% yield. This was followed by a sequence comprising the protection of the phenol group as a *t*-butyldimethylsilyl ether (TBS) and subsequent reduction of the methyl ester to the corresponding aldehyde using DIBAL-H, followed by deprotection with TBAF to furnish aldehydes **11–14** in 19–44% yield. The last step was to form the oxime function by condensation of the aldehyde with hydroxylamine. The desired oximes **15–18** were obtained in seven steps from **1** or **2** with an overall yield of 4–21%. Regarding the synthesis of oxime **19**, its preparation was reported earlier.^[17]



Scheme 1. Conditions and reagents: 1) Mesyl chloride (1.5 equiv.), Et₃N (3 equiv.), CH₂Cl₂, rt; 2) Amine RH **A**, **B**, or **C** (1 equiv.), K₂CO₃ (3 equiv.), CH₃CN, reflux; 3) H₂, Pd(OH)₂ (10% wt), EtOAc/MeOH (1/2), rt; 4) TBDMSCl (2.2 equiv.), imidazole (3 equiv.), DMF, rt, 2 h or TBDMSOTf (3 equiv.), 2,6-lutidine (3 equiv.), CH₂Cl₂, rt, 3.5 h; 5) DIBAL-H (2.5 equiv.), CH₂Cl₂, -78 °C, 15 min; 6) TBAF (1,1 equiv.), THF, rt, 1 h; 7) NH₂OH.HCl (1.2 equiv.), NaOAc (1.3 equiv.), EtOH, rt, 1 h

Reversible inhibition of hAChE and hBChE. We tested oximes **15–19** as reversible hAChE and hBChE inhibitors. Enzyme activity was measured in the presence of the substrate acetylthiocholine and in an oxime concentration range to determine the inhibition dissociation constant (K_i). All of the oximes inhibited both hAChE and hBChE in a range of micromolar concentrations (**Table 1**) like standard pyridinium and bispyridinium aldoximes (e.g., 2-PAM, HI-6).^[18] The highest inhibition of both hAChE and hBChE was observed for oximes **15** and **19** bearing a piperidine ring and a 1-(4-*N,N*-dimethylamino phenyl)-1,2,3,4-tetrahydroisoquinoline, respectively. It should be noted that all of these oximes – except compound **16** – inhibited both hAChE and hBChE with very similar potency. Thus, the selectivity for hBChE over hAChE was observed only for oxime **16** bearing a morpholine ring and the shortest linker (butyl). The affinities determined suggested that all of the tested oximes would bind to phosphorylated hAChE and hBChE, and hopefully reactivate them by nucleophilic displacement.

Oxime-assisted reactivation of OP-phosphylated hAChE and hBChE. We tested oximes **15–19** as reactivators of hAChE and hBChE inhibited by five OPs (VX, sarin, cyclosarin, paraoxon and tabun) and compared them to the standard reactivator, HI-6.^[16c, 19] The reactivation of phosphylated hAChE was evaluated over a wide oxime concentration range (**Figure S1**) enabling us to deconstruct reactivation constants (**Table 2**). The majority of the oximes reactivated all of the tested OP-inhibited hAChE to a high extent (i.e., 80-100 % of the enzyme activity). The most notable result was obtained for reactivation of VX-inhibited hAChE by oximes **16** and **17**, which displayed a ~2-fold higher maximal first-order reactivation rate constant (k_{+2}) compared to HI-6. The highest second order reactivation rate

Table 1. Dissociation inhibition constants ($K_i \pm$ S.E.) of hAChE and hBChE for oximes **15–19** determined from at least three experiments at 25 °C.

hAChE		hBChE	
Oxime	K_i (μ M)	Oxime	K_i (μ M)
15	10 \pm 1.5	15	9.8 \pm 3.0
16	135 \pm 14	16	46 \pm 20
17	168 \pm 23	17	170 \pm 15
18	37 \pm 1.1	18	33 \pm 1.2
19	5.4 \pm 1.2	19	2.3 \pm 0.5
HI-6	46 \pm 4.3	HI-6	420 \pm 100
2-PAM	210 \pm 45	2-PAM	140 \pm 16

constant of 30 800 M⁻¹min⁻¹ was obtained for oxime **18**, primarily due to its low dissociation constant ($K_{ox} = 10 \mu$ M). In the case of sarin, oximes **16**, **18** and **19** were the most potent reactivators when comparing the overall rate constants (k_i), but oxime **16** was the most effective one due to its high first-order reactivation rate (k_{+2}), while the potency of oxime **19** resulted primarily from its low dissociation constant (i.e., the highest affinity). The reactivation of cyclosarin-inhibited hAChE by oximes **15–18** terminated at 100%, but this level was reached much more slowly than for of HI-6 (**Table 2**). Interestingly, in the case of tabun, the 3-hydroxy-2-pyridine aldoximes reactivated 50-90 % of the phosphoroamidated hAChE conjugate known as particularly resistant to reactivation with the standard oximes. Again, oximes **16–18** were the most productive in nucleophilic displacement of phosphorus moiety, although the maximal

Table 2. Reactivation of OP-inhibited human AChE by oximes **15-19** and HI-6^[a]

OP	Oxime (μM)	k_{+2} (min^{-1})	K_{ox} (μM)	k_r ($\text{M}^{-1} \text{min}^{-1}$)	React _{max} (%)	t (min)
VX						
	15	0.17 ± 0.03	90 ± 30	1890 ± 410	90	30
	16	0.68 ± 0.07	300 ± 60	2270 ± 240	100	10
	17	0.57 ± 0.08	120 ± 50	4900 ± 1250	100	10
	18	0.31 ± 0.01	10 ± 3	30900 ± 8100	100	10
	19	0.07 ± 0.01	30 ± 10	2310 ± 650	90	60
	HI-6 ^[b]	0.33 ± 0.02	60 ± 10	5740 ± 1120	90	15
Sarin						
	15	0.075 ± 0.003	160 ± 20	490 ± 50	100	60
	16	0.29 ± 0.03	270 ± 90	1080 ± 290	100	10
	17	0.12 ± 0.01	220 ± 60	560 ± 130	100	30
	18	0.180 ± 0.005	130 ± 10	1380 ± 60	90	15
	19	0.019 ± 0.001	20 ± 5	1000 ± 220	80	>300 ^[c]
	HI-6	0.9 ± 0.1	170 ± 40	5420 ± 780	60-90	4
Cyclosarin						
	15	0.06 ± 0.01	330 ± 110	180 ± 40	100	60
	16	0.09 ± 0.01	430 ± 130	210 ± 40	100	45
	17	0.04 ± 0.01	120 ± 80	320 ± 140	100	100
	18	0.020 ± 0.006	120 ± 100	170 ± 90	100	120
	19 ^[d]	-	-	80 ± 3	80	>250 ^[c]
	HI-6 ^[d]	-	-	22100 ± 1300	100	<1
Tabun						
	15	0.0033 ± 0.0004	110 ± 40	30 ± 5	50	400
	16	0.016 ± 0.007	410 ± 280	40 ± 10	80	420
	17	0.014 ± 0.001	310 ± 100	45 ± 10	90	240
	18	0.014 ± 0.002	140 ± 60	100 ± 40	80	210
	19	0.0029 ± 0.0002	7.6 ± 2.5	390 ± 120	60	520
	HI-6	nd ^[e]	nd	nd	10	24 h
Paraoxon						
	15	0.07 ± 0.02	200 ± 110	340 ± 100	70	30
	16	0.36 ± 0.03	850 ± 150	430 ± 40	80	10
	17	0.27 ± 0.03	620 ± 180	440 ± 80	80	15
	18	0.24 ± 0.02	190 ± 70	1300 ± 350	80	10
	19	0.058 ± 0.006	30 ± 10	1800 ± 600	80	30
	HI-6	0.026 ± 0.001	590 ± 50	50 ± 2.2	90	170

[a] The maximal first-order reactivation rate constant ($k_{+2} \pm \text{S.E.}$), the overall second-order reactivation rate constant ($k_r \pm \text{S.E.}$), the phosphorylated enzyme-oxime dissociation constant ($K_{\text{ox}} \pm \text{S.E.}$), the maximal reactivation (React_{max}) and the time to maximal reactivation (t) were evaluated from at least three experiments at 25 °C; [b] from Maček Hrvat *et al.*^[16c]; [c] reactivation had not terminated at this time point; [d] linear dependence of k_{obs} vs. oxime concentration in the studied concentration range; [e] nd, not determined.

reactivation was achieved much more slowly than with other OPs. Oximes **15-19** were also evaluated for the reactivation of the diethyl phosphorylated hAChE conjugate obtained by inhibition of hAChE with paraoxon, the active metabolite of the insecticide parathion. In terms of the overall reactivation rate, k_r , the paraoxon-hAChE conjugate was the most productively

reactivated by oxime **19** as a result of its high binding affinity. All of the novel oximes reactivated the paraoxon-inhibited hAChE more potently than HI-6 primarily due to a higher k_{+2} (e.g., 15-fold higher for **16**). Moreover, in comparison with the other tested OPs, it seems that the tested 3-hydroxy-2-pyridine

aldoximes showed the largest improvement in reactivation over HI-6 for the diethyl phosphonylated hAChE.

In general, the reactivation of phosphylated hBChE still presents a challenge, since the standard pyridinium aldoximes are poor reactivators of hBChE, and only a few reactivators, recently described in the literature, exhibited promising potency for the reactivation of VX- and paraoxon-inhibited hBChE.^[13], 16d, 20] Reactivation of phosphylated hBChE was very efficient for

conjugates with cyclosarin, VX and paraoxon, but weak for sarin and tabun (**Table 3**). In terms of overall hBChE reactivation, out of the tested oximes, including HI-6, oxime **18** could be highlighted as the most potent reactivator of VX-, cyclosarin-, paraoxon- and tabun-inhibited hBChE. Oximes **15-19** were much better reactivators of paraoxon-inhibited hBChE than HI-6. For instance, the maximal reactivation rates of oximes **16, 17**

Table 3. Reactivation of OP-inhibited human BChE by oximes **15-19** and HI-6^[a]

OP	Oxime (μM)	k_{r2} (min^{-1})	K_{Ox} (μM)	k_r ($\text{M}^{-1} \text{min}^{-1}$)	React. _{max} (%)	t (min)
VX						
	15	0.05 ± 0.01	270 ± 150	180 ± 50	90	120
	16	0.10 ± 0.04	370 ± 240	270 ± 70	100	60
	17	0.059 ± 0.004	160 ± 40	360 ± 65	80	60
	18	0.096 ± 0.007	130 ± 30	760 ± 150	80	45
	19	0.020 ± 0.002	190 ± 40	110 ± 10	80	150
	HI-6 ^[b]	0.12 ± 0.03	370 ± 230	330 ± 230	85	120
Sarin						
	15	$0.0022 \pm 0.0005^{[c]}$	-	-	45	325
	16	$0.005 \pm 0.001^{[c]}$	-	-	90	325
	17	$0.0036 \pm 0.0004^{[c]}$	-	-	65	325
	18	$0.007 \pm 0.002^{[c]}$	-	-	80	325
	19	$0.0042 \pm 0.0005^{[c]}$	-	-	65	325
	HI-6	0.04 ± 0.02	270 ± 200	150 ± 40	100	300
Cyclosarin						
	15	0.32 ± 0.04	810 ± 200	390 ± 50	90	15
	16	0.5 ± 0.1	790 ± 420	610 ± 180	90	10
	17	0.39 ± 0.05	700 ± 190	560 ± 80	90	15
	18	0.32 ± 0.07	330 ± 140	980 ± 210	90	15
	19	0.11 ± 0.03	160 ± 70	710 ± 150	90	60
	HI-6 ^[d]	-	-	780 ± 30	90	30
Tabun						
	15	nd ^[e]	nd	nd	< 10	24 h
	16	nd	nd	nd	< 10	24 h
	17	nd	nd	nd	< 20	24 h
	18	0.004 ± 0.001	540 ± 290	7.9 ± 2.8	40	24 h
	19	nd	nd	nd	< 25	24 h
	HI-6 ^[f]	0.0016 ± 0.0004	1800 ± 1000	0.91 ± 0.57	25	18 h
Paraoxon						
	15	0.020 ± 0.003	140 ± 40	140 ± 30	90	270
	16	0.15 ± 0.02	1160 ± 310	130 ± 20	90	40
	17	0.056 ± 0.006	250 ± 80	230 ± 50	100	90
	18	0.075 ± 0.01	290 ± 110	260 ± 70	100	90
	19	0.023 ± 0.008	640 ± 280	35 ± 4	80	270
	HI-6	0.0068 ± 0.0004	450 ± 70	15 ± 2	80	500

[a] the maximal first-order reactivation rate constant ($k_{r2} \pm \text{S.E.}$), the overall second-order reactivation rate constant ($k_r \pm \text{S.E.}$), phosphylated enzyme-oxime dissociation constant ($K_{Ox} \pm \text{S.E.}$), maximal reactivation (React._{max}) and the time to maximal reactivation (t) were evaluated from at least three experiments at 25 °C; [b] from Katalinić *et al.*^[20a]; [c] the observed first-order reactivation rate constant, k_{obs} (min^{-1}) \pm S.D., at a given oxime concentration; [d] linear dependence of k_{obs} vs. oxime concentration; [e] nd, not determined; [f] from Lucić Vrdoljak *et al.*^[21]

and **18** were up to 22-fold higher than those of HI-6. Much like as in the case of hAChE reactivation, oxime **16** had the highest k_{42} , showing its versatility and potency to effectively reactivate the cyclosarin, VX and paraoxon conjugates of hBChE. It should also be emphasized that for cyclosarin, the evaluated k_{42} values for all tested oximes were at least 5-fold higher for hBChE than those for hAChE (cf. **Table 2**). However, the binding affinities of oximes **15-19** were not good enough for them to be promising reactivators of cyclosarin-inhibited hBChE. Indeed, all of the evaluated dissociation constants for reactivation of hBChE were generally higher than the ones determined for hAChE. Therefore, it seems that low binding affinity, which possibly results from the greater flexibility and conformational freedom of oximes due to a more voluminous hBChE active site than that of hAChE, is a major obstacle in the search for an efficient reactivator of hBChE.

Scavenging of OPs with oximes in whole human blood. The results obtained for reactivation of OP-inhibited cholinesterases by the most potent reactivators directed our research towards oximes **16** and **18** as a potential oxime-assisted catalytic bioscavenger. These two oximes were chosen as representatives of potent reactivators with high reactivation efficiency and high binding affinity, respectively. To be more precise, these oximes and native cholinesterases in whole blood could establish the catalytic cycle of OPs hydrolysis by rapid conjugation of OP with both erythrocyte AChE and plasma BChE followed by enhanced oxime-assisted hydrolysis of the

OP-enzyme conjugates. The maximal achieved recovery of total cholinesterase activity is proof of complete OP degradation (i.e., there is no more OP available for cholinesterase inhibition). Hence, we tested the *ex vivo* degradation of VX, sarin, cyclosarin and paraoxon in human whole blood (hWB) by measuring the recovery of total cholinesterase activity upon cycles of inhibition by OP and reactivation with oxime **16** and **18** (**Figure 4**). Oxime **16** recovered more than 80% of total cholinesterase activity within 5–15 min (depending on the OP excess), except for cyclosarin where it took 60 min for the activity recovery regardless of the OP concentration. Slower recovery of total activity observed for cyclosarin can be explained by poor *in vitro* reactivation of the cyclosarin-inhibited hAChE (cf. **Table 2**) and the fact that 80% of total cholinesterase activity in the hWB originates from hAChE. In the case of a 50-fold excess of paraoxon, lower recovery (40%) of total cholinesterase activity was observed. In comparison to oxime **16**, oxime **18** recovered activity much more slowly, reaching its maximum in 40–60 min in the case of all OPs as expected from lower maximal reactivation rate constants, k_{42} (cf. **Table 2** and **3**). Scavenging of paraoxon and cyclosarin by oxime **18** ended at 40–60% and 40% of total activity, respectively. Although we cannot offer an explanation, it is interesting to note that the activity recovery with oxime **18** in the case of sarin and cyclosarin and oxime **16** and cyclosarin was not related to the OP concentration.

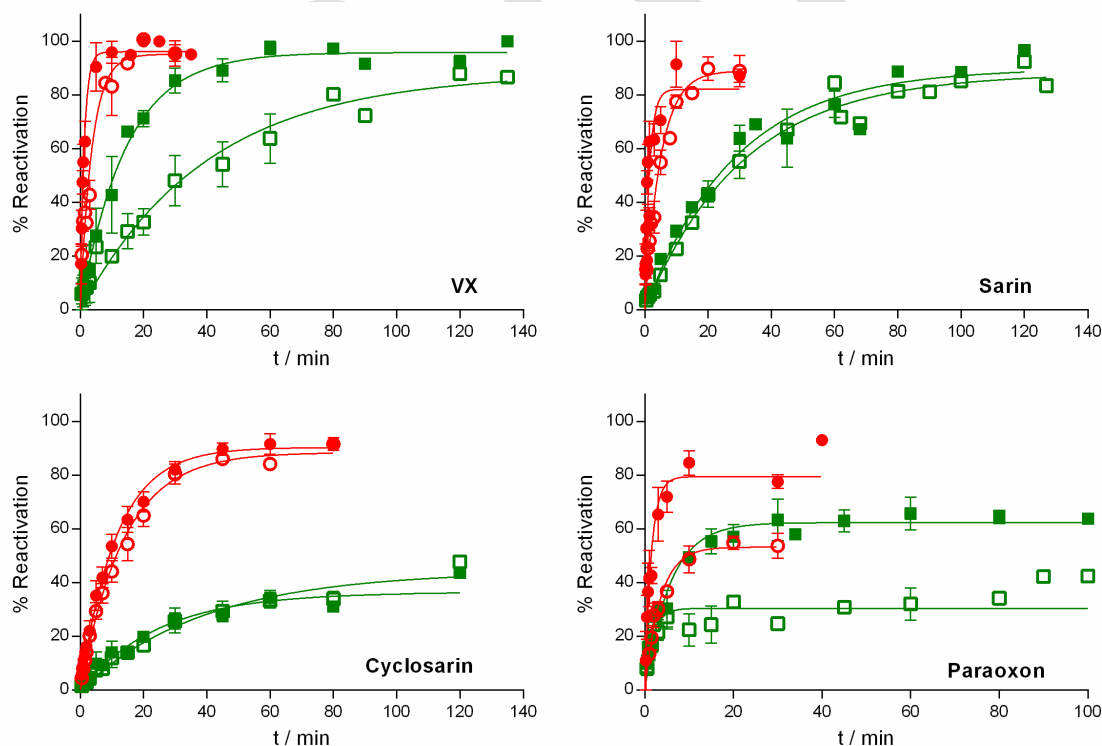


Figure 4. Recovery of total cholinesterase activity in whole human blood during scavenging of OPs (0.7 μM , full symbols and 3.4 μM , empty symbols) with oxime **16** (red) and **18** (green). Mean of at least 3 experiments \pm SEM is presented.

Crystal structure of the complex of oxime 17 with TcAChE.

To understand how a representative oxime of the 3-hydroxy-2-pyridine aldoxime group binds within the active site of AChE, we determined the crystal structure of the complex of oxime **17** with TcAChE (PDB ID: 6EWK). **Figure 5** shows the reactivator bound within the TcAChE active-site gorge in a productive conformation capable of a nucleophilic attack on an OP moiety covalently attached to catalytic Ser200. The morpholine group of **17** is bound to the peripheral anionic site (PAS) of TcAChE, stabilized by interaction with Trp279 (equivalent to Trp286 in hAChE). Its binding at the PAS induces re-arrangements in the side chains of Tyr70 and Gln74 (Tyr72 and Leu76, respectively, in hAChE). The oxime moiety is located at the active site, being stabilized by an H-bond with H₂O 14, and pointing towards catalytic Ser200 (Ser203 in hAChE) at a distance of 3.5 Å. The oxime moiety is also stabilized by a polyethylene glycol (PEG) molecule from the crystallization solution located between the aromatic ring of **17** and Trp84 (Trp 86 in hAChE). Comparison with the apo TcAChE structure indicates that the 3-hydroxy-2-pyridine aldoxime moiety displaces residues Phe330, Phe331 and His440 from their apo conformation (not shown). Superposition with the crystal structures of the sarin-hAChE (PDB ID: 5FPQ)^[22] and VX-TcAChE (PDB ID: 1VXR)^[23] conjugates shows that **17** could bind to phosphorylated hAChE in the same active orientation as seen in the crystal structure of the **17**/TcAChE complex. *In vivo*, in the absence of PEG, the oxime could oscillate between various conformations as

observed in other crystal structures of complexes of oximes with AChE (e.g., bis-imidazolium oxime; PDB ID: 5BWB),^[24] bis-pyridinium oxime ortho-7; PDB ID: 5BWC).^[24] In complexes of other oximes with AChE, a conformational change in the side chain of Trp279 (Trp286 in hAChE) was reported.^[24] However, in the **17**/TcAChE complex, the Trp279 side chain retains its apo conformation.

The specific binding of the morpholine portion of **17** to the peripheral site confers it an advantage compared to 2-PAM, which binds only to the catalytic site stabilized by π - π interactions with Trp84 (Trp86 in hAChE) and that the oxime points to the opposite of the catalytic serine either phosphorylated or not (PDB ID 2VQ6; PDB ID: 2WG1).^[25] Oxime **17** is anchored in a productive conformation directing the oxime to the catalytic serine, increasing the probability that reactivation occurs, HI-6 also binds to the peripheral site, as crystal structures have shown, however because of its lower K_i (five times lower than that determined for **16** and **17**) it is also a high affinity inhibitor, a non-desired characteristic for AChE's reactivators. Even higher K_i values were determined for compounds 15, 18 and 19 suggesting a different binding from 16 and 17 (see next section), either with additional interactions at the catalytic site or in analogous way to HI-6 by stabilizing an alternative conformation Trp279 (Trp286 in hAChE) at the peripheral site, being sandwiched between the indole group of the tryptophan and Tyr70 (Tyr72 in hAChE).

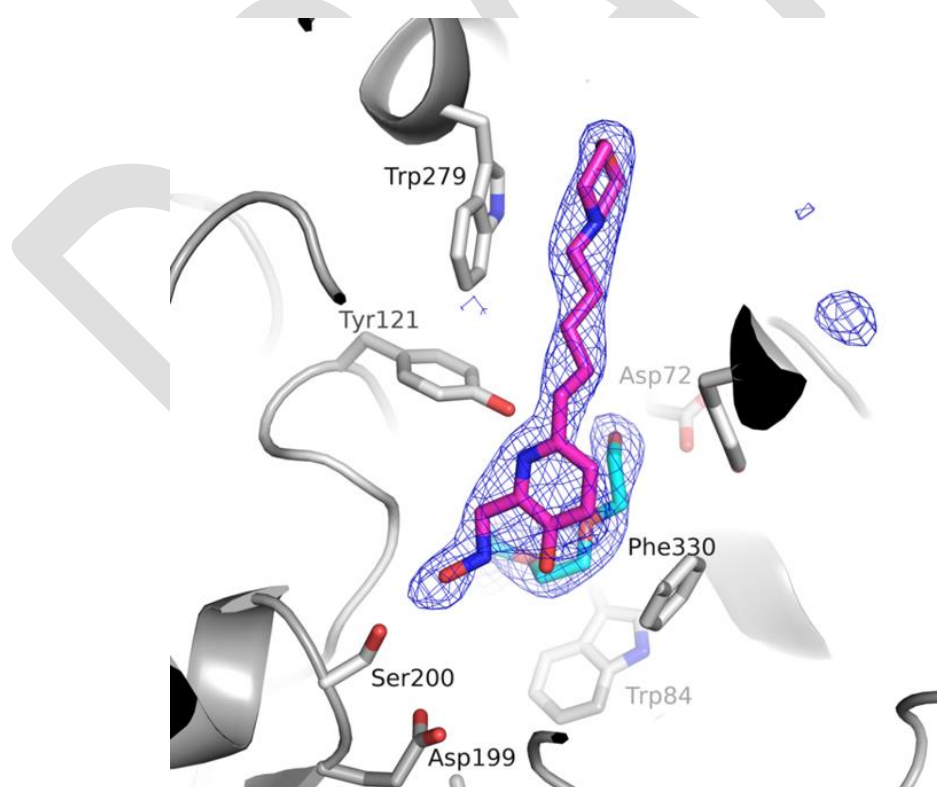


Figure 5. Crystal structure of the **17**/TcAChE complex. The oxime moiety is at 3.5 Å from Ser200O_y. The omit map Fo-Fc (blue mesh), shown around oxime **17** (magenta) and a PEG molecule (cyan) positioned between the oxime and Trp84 (not shown), is contoured at 3.5 σ .

Docking of oximes into TcAChE, and VX-mAChE and cyclosarin-hBAChE. Prior to docking analysis, we performed the amino sequence alignment of TcAChE, mouse AChE (mAChE) and hAChE. **Figure S3** shows that, along with high indices of sequence identity (55.3%) and similarity (76.1%) there is a 92.9% identity in the active site domains such as the catalytic site, oxyanion hole, acyl pocket, choline-binding pocket of the active site, and the PAS.

We superimposed the crystal and model structures of TcAChE and mAChE with oximes (**Figure 6**) to (a) analyse a model structure of the complex of **17** and apo TcAChE for comparison with other molecular docking structures, (b) analyse how the conjugated OP moiety changes the binding mode of an oxime, and (c) reveal the nonbonding interactions in complexes that could be related to the reactivation efficacy of the oximes. The superposition of the crystal structure of the **17/TcAChE** complex (cf. **Figure 5**) and its molecular docking model obtained by docking of **17** into the crystal structure (PDB ID: 6EWK) after the

removal of both the oxime and the PEG molecule (**Figure S3**) showed that, in both structures, **17** has the same orientation, with its morpholine ring within the PAS, and its 3-hydroxy-2-pyridinealdoxime moiety directed towards the catalytic site. The major difference is a ~ 4 Å deeper positioning of the docked **17** within the active-site gorge, which in turn prevented the stabilisation of the morpholine group by interactions with Trp279 that resulted in multiple T-shaped π - π interactions between the 3-hydroxy-2-pyridinealdoxime moiety and Trp84 and His440, and shortened the distance between the oxime moiety and Ser200 γ to only 2.6 Å (**Figure 6A, Table S4**). It seems that the PEG molecule present in the crystal structure largely predetermines the binding mode of **17** in the active-site gorge in the TcAChE crystal structure. To examine the oxime's binding modes in phosphorylated AChE, we superimposed the model structure of **17** docked into the TcAChE crystal structure (cf. **Figure S3**) and the model obtained by docking it into the crystal structure of VX-inhibited mAChE (PDB ID: 2Y2U; **Figure 6B**).^[26]

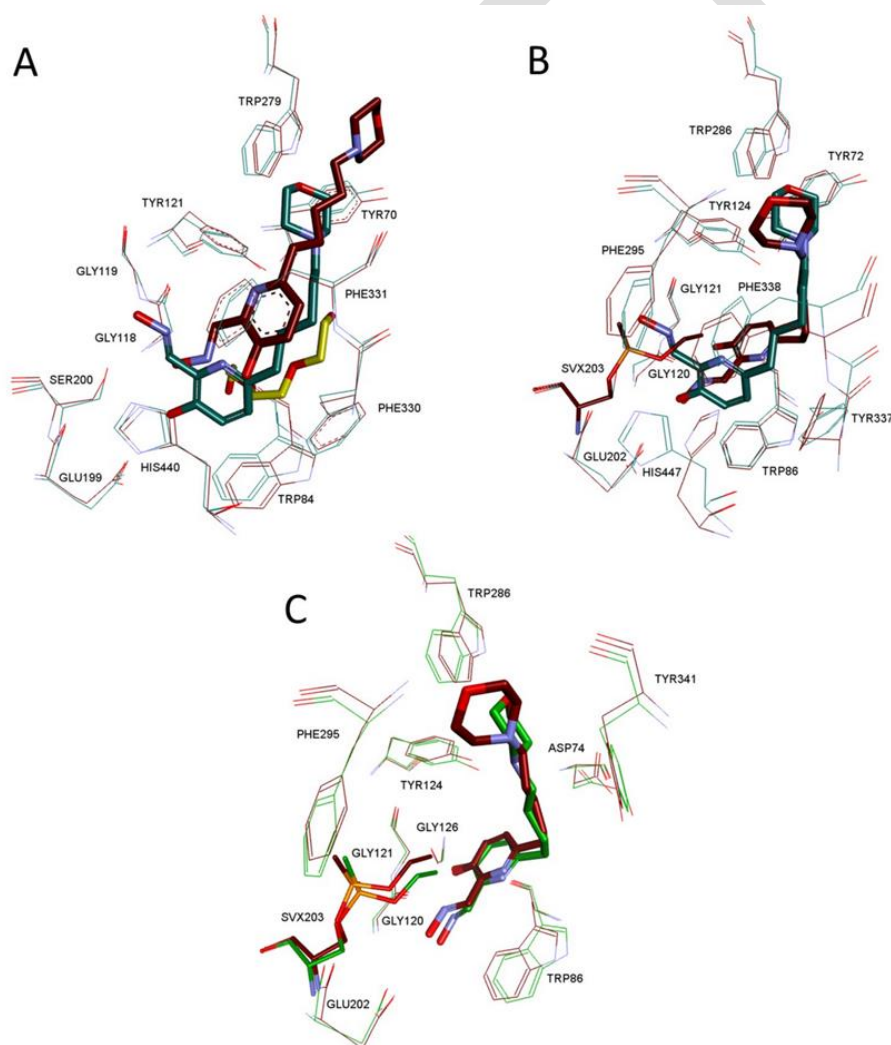


Figure 6. Superposition of A) The crystal structure of the **17/TcAChE** complex (carbon atoms shown in purple) and the model structure of the complex **17** with apo TcAChE (6EWK once the oxime and PEG were omitted) (carbon atoms shown in dark green); B) The model structures of **17** bound to apo TcAChE (purple) and VX-mAChE conjugate (dark green); C) The model structures of the VX-mAChE conjugate complexed with **16** (green) or **17** (purple). Oxygen atoms are shown in red, nitrogen atoms in cyan, and the phosphorus atoms in orange.

As one might expect, the steric hindrance between the ethyl moiety of the conjugated VX and the oxime moiety obstructed binding of **17** in the orientations observed in the crystal structure of TcAChE (**Figure 5**) or predicted by docking (**Figure 6B**). The superimposition of model structures of oximes **16** and **17** docked into VX-inhibited mouse AChE presented in **Figure 6C** showed that both oximes are bound in an elongated conformation with their 3-hydroxy-2-pyridinealoxime moieties within the active site, forming a π - π interaction with Trp86 in the choline binding site, as has been shown for numerous compounds containing aromatic moiety,^[27] including bispyridinium oxime reactivators (e.g., HI-6; PDB: 5FPP), when bound in a non-productive orientation in phosphorylated mAChE.^[22] Although the distance between the oxygen atom of the oxime group and the phosphorus atom (6.59 Å for oxime **16**, 5.49 Å for oxime **17**) is close to optimal (4–5 Å) for a nucleophilic attack on the P=O moiety,^[28] both lack the optimal orientation of the oxime group for an in-line nucleophilic attack (i.e., the oxime group does not approach the P=O moiety at an angle of approximately 180° to the leaving group).^[29] The only difference in the positioning of the two oximes is in the orientation of the morpholine ring, implying that the higher reactivation efficiency (in terms of k_r) of oxime **17** over **16** could result from a better stabilisation of **17** in the productive conformation. Indeed, while both oximes make the above-mentioned π - π interaction with Trp86, and the π -cation interaction with peripheral Tyr341 through their protonated morpholine nitrogens, the total number of H-bonds between the oxime and the surrounding amino acids is higher for **17** than for **16** (9 vs. 7; **Table S4**). This evaluation is in accordance with the kinetic parameters for the two oximes determined for the reactivation of VX-inhibited hAChE (cf. **Table 2**). Thus, while they have a similar k_{+2} constant, K_{OX} is almost 3-fold smaller for **17** than for **16**, which might reflect the observed difference in the non-bonding interactions of their morpholine moiety and the higher number of H-bonds in the case of **17**.

The molecular modelling of the complex of hBChE with oxime **16** was performed with the objective to examine the binding mode of **16**, which displays the highest reactivation efficiency in terms of k_{+2} (cf. **Table 2** and **3**). We modelled two structures of the complex that display different conformations of the cyclosarin moiety, in terms of torsion angle around single P–O-isopropyl bond, which resemble those observed for the isopropyl group of the sarin in the crystal structure of a complex of HI-6 with the sarin-AChE conjugate (PDB ID: 5FPP)^[22] The resulting model structures are superimposed as shown in **Figure 7**. When **16** was docked in the active site of hBChE conjugated with cyclosarin in the predominant conformation (i.e., analogous to the predominant conformation in the sarin/hBChE),^[22] **16** bound in the centre of the active site, in a bent conformation, with the morpholine moiety positioned above the choline binding site; the 3-hydroxy-2-pyridinealoxime group was positioned above the oxyanion hole, adjacent to the acyl binding pocket, while the alkyl linker was bent upwards towards the entrance of the gorge (**Figure 7**). The morpholine ring is stabilized by an electrostatic interaction between its protonated nitrogen and the Asp70 carboxyl, and by multiple H-bonds. Moreover, the distance and orientation of the oxime of the 3-hydroxy-2-pyridine aldoxime

moiety is optimal for an in-line nucleophilic attack on the phosphorus atom.^[28-29] Surprisingly, when **16** is docked in the active site with cyclosarin moiety in the alternative conformation, the binding mode of oxime **16** changes only slightly, predominantly in the alkyl linker, as compared to its binding mode in the model with predominant conformation. Both the morpholine ring and the 3-hydroxy-2-pyridinealoxime moiety largely maintain their positions, so that the oxime group is still optimally positioned in the productive conformation (**Figure 7**). It thus seems that the high k_{+2} observed for the reactivation of cyclosarin-inhibited BChE could, at least partly, be a result of the ability of oxime **16** to bind in the productive conformation regardless of the dynamics of the conjugated cyclosarin moiety. Detailed information concerning the non-bonding interactions of oxime **16** within the active site of cyclosarin-inhibited BChE is supplied in the Supporting Information (**Table S4**).

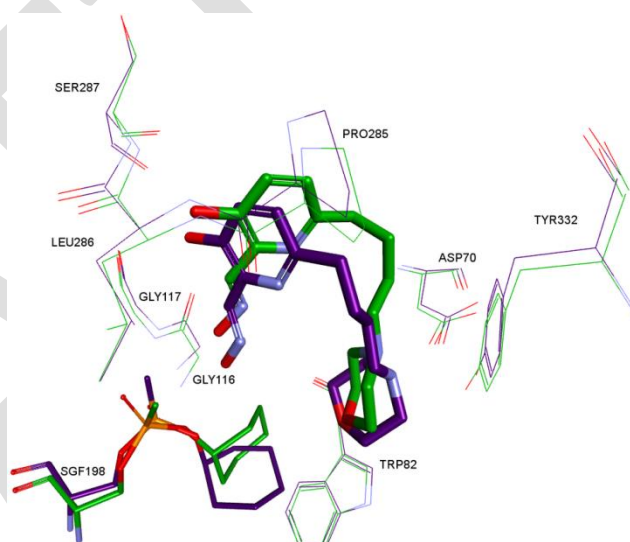


Figure 7. Superposition of model structures of the complex of lead oxime **16** and the cyclosarin-hBChE conjugate with a predominant conformation of the cyclosarin moiety (green) or an alternative conformation (purple). Oxygen atoms are shown in red, nitrogen atoms are shown in cyan, and the phosphorus atom in orange.

In silico and in vitro determination of pK_a values. Molecular properties of oximes in terms of their pK_a values were analysed both *in silico* and *in vitro* to estimate their acid/base character and predict their propensity to penetrate the BBB (**Table 4**). *In silico* tests predicted the existence of up to 14-15 possible microspecies for oximes **15–18**, and 18 microspecies for oxime **19**, in the pH range of 0-14 depending upon the ionization status of four or five functional groups. Accordingly, the oxime absorbance scans at various pH values showed several absorption maxima in the range studied (**Figure 8**), with those at 315 and 360 nm assumed to correspond to the absorption of species with a protonated (=N–OH) and a deprotonated oxime group (=N–O⁻), respectively.^[30] Therefore, pK_a values were determined from the absorption peak at 360 nm alone due to a bathochromic shift of the absorption maximum from 314 nm at pH 4.5 to 329 nm at pH 9.1 (**Figures 8** and **S5**). A similar shift

for 2-trimethylammonio-6-hydroxybenzaldehyde oximes was reported previously by Radić *et al.*^[16d] Two dissociation constants were observed for oximes **16** and **18** in the pH range studied, most likely corresponding to the dissociation of the oxime group (=N-OH) and the hydroxyl group (-OH) on the pyridinium ring, since the absorption at 360 nm was presumed to originate from $\pi \rightarrow \pi^*$ transitions within the pyridinium aromatic system.^[31] Since strong isomerization of the oxime group is expected only in a strong acidic environment,^[32] only spectra measured in solutions of pH ≥ 6 were studied. Due to its low solubility, *in vitro* evaluation of pK_a values for oxime **19** was not possible. As presented in **Table 4**, there is good correlation between the *in silico* prediction and the *in vitro* determination of pK_a values (i.e., for the pK_a values of the oxime group (compounds **15–18**) and for the hydroxyl group (compounds **16** and **18**) on the pyridine ring). Therefore, it could be expected that, at physiological pH, the tertiary amine of these oximes is mostly protonated ($R_3\text{-NH}^+$ group), while oximes **16** and **17** have the highest level of non-ionized species (20–30%) and would thus be expected to cross the BBB at a higher rate.

Furthermore, the oxime group of compounds **15–19** is mostly protonated at pH 7.4 (around 80%) according to both *in silico* and *in vitro* evaluation. It should be noted that their pK_a values for the oxime group are in the range of standard pyridinium oximes: higher than the one of the *ortho*-pyridinium oxime HI-6 ($pK_a = 7.47$) and lower than for the one of *para*-pyridinium oxime TMB-4 ($pK_a = 8.39$).^[30]

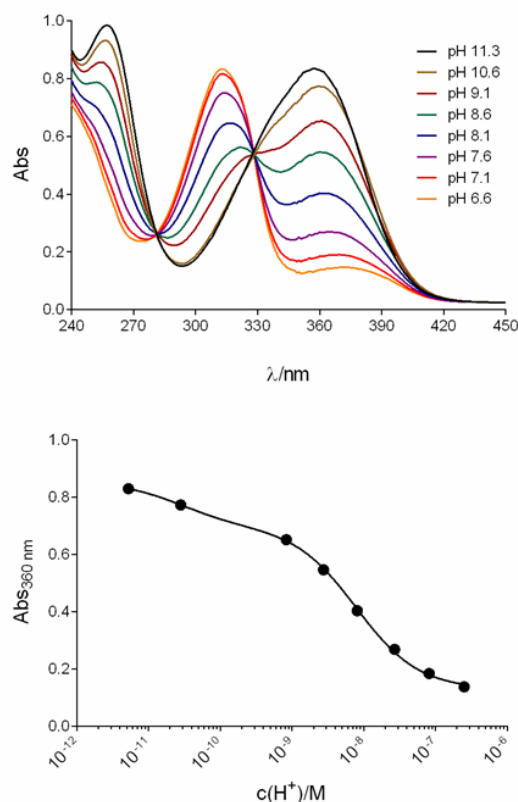


Figure 8. A) Absorption spectra at various pH values obtained for 100 μM **16** (at 25 °C) and B) pH-dependent absorbance change at 360 nm.

Table 4. Dissociation constants, pK_a , for the oxime group (=N-OH), the hydroxyl group (-OH), the nitrogen atom (R=N-R') in the pyridinium ring, and the tertiary amine of the substituent ($R_3\text{-NH}^+$)

Oxime	<i>In silico</i> pK_a				<i>In vitro</i> pK_a (360 nm) ^a	
	=N-OH	-OH	R=N-R'	$R_3\text{-NH}^+$	pK_{a1}	pK_{a2}
15	8.10	9.82	3.41	10.49	8.01 ± 0.04	nd ^b
16	8.33	10.33	3.29	7.32	8.08 ± 0.04	10.53 ± 0.21
17	8.37	10.33	3.41	7.50	8.03 ± 0.06	nd
18	8.52	10.33	3.44	7.89	8.20 ± 0.06	10.44 ± 0.27
19 ^c	10.34	8.90	3.35	7.82	-	-

^a mean \pm S.E determined at 25 °C; ^b nd, not determined; ^c *in silico* evaluation predicted for **19** an additional dimethyl tertiary amino group with $pK_a = 4.17$

In silico prediction of BBB penetration. Other than the ionization status of molecules, there are some general molecular descriptors that are important in the evaluation of the BBB permeability potential (recommended by Pajouhesh and Lenz).^[33] **Figure 9** shows the radar plot of such physicochemical properties of oximes **15–19** in relation to the properties of CNS-active drugs, which generally have lower molecular weight (MW<450), have moderate hydrophobicity ($\log P < 5$), have fewer hydrogen bonds and acceptors (HBD< 3 and HBA<7), fewer rotatable bonds (RB<8) and are less polar (polar surface area PSA<70 Å²) than drugs that are not CNS-active.^[33] All of them, except **19**, have optimal values of lipophilicity ($\log P = 0.9\text{--}4.6$) and molecular weight (280–400), and optimal numbers of H-bond donors (2) and H-bond acceptors (5–7). Molecular

flexibility, as characterized by the number of rotatable bonds (6–9), is favourable in three out of five oximes. Also, the pK_a of the most basic group (i.e., the $R_3\text{-NH}^+$ group; c.f. **Table 4**) is in or almost in the recommended range (7.5–10.0) for oximes **16–19**. The only shortfall for this group of oximes is a higher polar surface area (78–87 Å²), except for oxime **15** (69 Å²). Using the algorithm described by Wager *et al.*^[31, 34] the central nervous system multi-parameter optimization score was calculated based on the six fundamental physicochemical parameters ($\log P$, $\log D$, pK_a , HBD, PSA, MW) where the score for CNS candidates should be ≥ 4 (scale 0–6). Oximes **15–18** are all scored favourably, in the order: **16** (5.5) = **17** (5.5) > **15** (4.5) = **18** (4.5) > **19** (2.1).

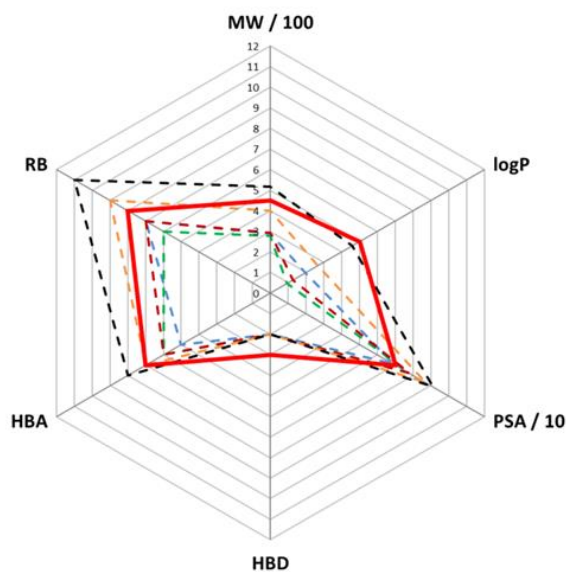


Figure 9. Radar plot of physicochemical properties (molecular weight, MW; lipophilicity coefficient, logP; number of hydrogen bonds donors, HBD, and acceptors HBA; rotatable bonds, RB; polar surface area, PSA) of the oximes **15** (blue), **16** (green), **17** (dark red), **18** (orange), **19** (black) and upper recommended values for the CNS-active drugs (full red line)

In vitro determination of BBB penetration for oximes. Brain penetration of the candidate oxime reactivators by passive diffusion was evaluated using the parallel artificial membrane permeation assay (PAMPA-BBB). The *in vitro* permeability (P_e) of the oximes through a lipid extract of porcine brain was determined using phosphate-buffered saline (PBS)/EtOH 70:30. Assay validation was carried out by comparing the experimental and literature permeability values of 14 commercial drugs (see SI), which gave a good linear correlation: P_e (exp) = 1.4525 P_e (lit) - 0.4926 ($R^2 = 0.9199$). Using this equation and the limits established by Di et al. for BBB permeation,^[35] the following ranges of permeability were established: P_e (10^{-6} cm s^{-1}) > 5.3 for compounds with high BBB permeation (CNS+), P_e (10^{-6} cm s^{-1}) < 2.4 for compounds with low BBB permeation (CNS-), and $5.3 > P_e$ (10^{-6} cm s^{-1}) > 2.4 for compounds with uncertain BBB permeation (CNS±). According to the PAMPA assay and results given in **Table 5**, passive transport across the BBB was observed for all of the tested oximes. For comparison, the standard oximes HI-6 and 2-PAM were shown to be impermeable with a similar PAMPA assay.^[36]

Table 5. *In vitro* brain permeability ($P_e \pm$ S.E.) of oximes 15–19 determined by the PAMPA-BBB assay (CNS+: high BBB permeation).

Oxime	P_e (10^{-6} cm s^{-1})
15	30.1 ± 5.5 (CNS+)
16	6.1 ± 0.5 (CNS+)
17	8.1 ± 0.31 (CNS+)
18	12.1 ± 1.9 (CNS+)
19	12.8 ± 1.5 (CNS+)

Discussion

Our study included reactivation measurements of both hAChE and hBChE inhibited by nerve agents, VX, sarin, cyclosarin and tabun, and paraoxon, the active metabolite of a pesticide parathion, along with a structural study and initial assessments of their CNS penetration. All five oximes, 3-hydroxy-2-pyridine aldoximes, though devoid of a permanent cationic charge, showed a moderate to high binding affinity for cholinesterases meaning that the activity of hAChE and hBChE is reversibly inhibited by the oximes. Moderate binding affinity towards the uninhibited enzyme is an indication for potential reactivators that have the best chance of productive interaction with OP-hAChE conjugates. Considering the results shown in **Table 1**, compounds **16** and **17**, exhibited the closest K_i to standard oximes (e.g., HI-6) towards hAChE and hBChE. It seems that the formation of protonation equilibria around two physiologically relevant ionisable groups in those oxime structures, an oxime group and a tertiary amine group, results in the coexistence of charged and uncharged reactivator species around physiological pH values. While cationic species have the best chance of productive interaction with OP-hAChE conjugates, the uncharged species can be expected to cross the blood-brain barrier delivering a reactivator into CNS. In addition, the combination of *in silico* prediction of BBB penetration and *in vitro* PAMPA assay highlighted compounds **16** and **17** as the most suitable to efficiently cross the BBB (**Figure 9**). Indeed, its high CNS-MPO scores (5.5 out of 6) predicted a very good brain penetration. Moreover, pK_a values (**Table 4**) showed that compounds **16** and **17** had the highest level of uncharged species (20–30%) and would thus be expected to cross the BBB at a higher rate compared to oximes **15**, **18** and **19**. Additionally, the tertiary amine moieties that is positively charged at pH 7–8, as is the case for oximes **15–18**, can interact with negatively charged lipids of the membrane and the ionised form is then destabilised in the membrane which results in a decrease of the pK_a value and increase in the non-ionized form that is again reprotonated after crossing the membrane.^[14] All of these data suggested that compounds **16** and **17** have the best physicochemical properties to enter into the brain by passive transport. However, it should be kept in mind that the oxime concentration in the brain *in vivo* may be additionally influenced both by active transporters and efflux pumps widely present in the BBB.^[37] Nevertheless, it is anticipated that these 3-hydroxy-2-pyridine aldoximes will achieve brain concentrations higher than 10% of their blood concentrations, which is the reported upper limit for the standard oximes.^[38]

From the structure-activity relationship (SAR) perspective, the most important structural element governing reactivation efficiency of tested oximes is its moiety that supposed to be stabilised with residues from the peripheral site. A detailed examination of **Table 2** and **Table 3** drew our attention to oximes **16** and **17** both having a morpholine ring, which is stabilised in the peripheral site as observed in the crystal structure of AChE-**17** – and corroborated by docking for **16** – enabling a proper position of the 3-hydroxy-2-pyridine aldoxime moiety for nucleophilic displacement, regardless of the different

steric shield provided by OPs. Oxime **16** had the highest first-order reactivation rate (k_{+2}) for all OP-inhibited hAChE and OP-inhibited hBChE, and stood out as an effective reactivator at higher oxime concentrations, since it exhibited the lowest binding affinity towards OP-inhibited enzymes. Our results showed a reversible binding leading to progressive reactivation is thus facilitated by a pentyl linker (all oximes except **16**), while the optimal geometry of AChE-OP-oxime transition state is achieved with a butyl linker (only oxime **16**). In other words, the increase in the length of an alkyl linker (i.e., oxime **17**) slightly reduces an oxime's efficiency against all OPs. The higher *in vitro* overall reactivation rate of **17** out of all OP-inhibited hAChE and hBChE (except for sarin-inhibited hAChE) is therefore largely a reflection of its improved molecular recognition (i.e., better binding to OP-hAChE conjugates as indicated by smaller K_{OX} constants), while maintaining similar k_{+2} constants, in comparison to oxime **16**. Oximes **18** and **19** with more complex structures exhibited the highest binding affinity towards phosphorylated hAChE. Consequently, **18** showed good potencies to reactivate the VX and sarin-phosphorylated hAChE, while oxime **19** was potent reactivator of the tabun- and paraoxon-inhibited hAChE. A recent paper by Soukup *et al.* reported a correlation between high binding affinity and high cytotoxicity of compounds similar to **18** and **19**, although the mechanism is unclear.^[39] Thus, our data show the complexity of the reactivation and point to the properties that an efficient reactivator should have – not only a proper binding affinity for the phosphorylated cholinesterase but also an orientation that directs the oxime group towards phosphorylated serine within the active-site gorge. Besides, the resolution of the complex of TcAChE with compound **17** confirmed a productive conformation within the active site of the enzyme and showed the productive orientation of the oxime function toward the catalytic serine. Nevertheless, it is important to note that the structural diversity of OP-hAChE conjugates was not reflected in reactivation trends because these morpholine-3-hydroxy-2-pyridine aldoximes conjugates efficiently reactivated hAChE inhibited by all five tested OPs; thus, their structural features could be highlighted as important for developing potentially universal reactivators of phosphorylated ChEs. Oxime structure requirements for an efficient reactivation of hBChE, while structurally and functionally a very close relative of hAChE, are clearly different (Table 1 and Table 2) showing that relatively moderate variations of the active centre gorge size and shape in two enzymes have substantial consequences for forming a productive complementary fit of small reactivator molecules into OP conjugated enzymes. However, the case of OP-inhibited hBChE once again postulates that the combination of morpholine ring as peripheral site moiety and butyl linker (oxime **16**) gives the most efficient oxime (in terms of k_{+2}) against all OPs used except sarin, pointing out this combination as a possible property of an all-round reactivator. Therefore, oxime **16** showed the most optimal geometry of the hBChE-OP-oxime transition state and productive reactivation. An increase in the length of the alkyl linker again reduces the oxime's efficiency indicating that greater flexibility and conformational freedom of oxime **17**'s alkyl linker, permitted by a more voluminous hBChE

active site, cannot compensate for the initial directing properties of the butyl linker.

A practical outgrowth of our results is the application of these oximes in combination with native erythrocyte hAChE and plasma hBChE enzyme to catalyse the hydrolysis of organophosphates shown in the *ex vivo* scavenging assay that serves the purpose of evaluating reactivator's efficiency in *in vivo* resembling conditions (e.g., the presence of plasma proteins, presence of both AChE and BChE, etc.) and general scavenging potential of OPs in blood before they reach the synaptic AChE. Cholinesterases in the plasma are efficient scavengers of organophosphates in terms of reactivity, however their capacity is limited by virtue of the 1:1 stoichiometry between the small organophosphate (100 – 200 D) and the ~ 70 kD subunit bearing the catalytic serine. Hence, an enzyme-reactivator combination catalytic to the organophosphate hydrolysis, rather than stoichiometric to conjugation, would greatly reduce doses needed for scavenging. The degradation of OPs in whole human blood observed with both oximes (**16** and **18**) represents a significant improvement compared to some of our previous *ex vivo* studies,^[12, 16c, 20a] in which any significant scavenging effect was observed only when the blood was supplemented with suitable hAChE mutants or hBChE. Due to the financial costs of generating such exogenous enzymes, their short circulation time and the immunity challenges that arise, the design of oximes with an ability to reactivate native AChE and/or BChE effectively provides a much more desirable approach.

Conclusions

The novel class of oximes presented here showed an improvement in reactivation potency for VX-, paraoxon-, and tabun-phosphorylated hAChE when compared to the standard oxime HI-6. Oximes **16** and **17** appeared to be the most effective candidates with a broad spectrum of reactivation. Moreover, these oximes showed an exceptional potential for reactivation of cyclosarin-inhibited hBChE. The resolution of TcAChE in complex with oxime **17** displayed a productive conformation that could explain the promising potency to reactivate both phosphorylated hAChE and hBChE. Furthermore, oximes **16** and **17** are predicted to efficiently cross the BBB based both on *in silico* predictions and on the *in vitro* brain membrane permeability test. They could, therefore, potentially achieve significant concentrations both at the neuromuscular junction and in the brain. This, in turn, could result in an overall improved therapeutic outcome after OP poisoning.

Experimental Section

Chemistry. Solvents were purified by a dry solvent station MB-SPS-800 (MBraun) immediately prior to use. Triethylamine was distilled from CaH₂ and stored over BaO or KOH. All reagents were obtained from commercial suppliers (Sigma Aldrich, Acros, TCI) unless otherwise stated. Column chromatography purifications were performed on silica gel (40–63 μm) from Macherey-Nagel. Thin-layer chromatography (TLC) was carried out on Merck DC Kieselgel 60 F-254 aluminium sheets.

Compounds were visualized by UV irradiation and/or spraying with a solution of potassium permanganate, followed by charring at 150 °C. ¹H and ¹³C NMR spectra were recorded with a Bruker DPX 300 spectrometer (Bruker, Wissembourg, France). Chemical shifts are expressed in parts per million (ppm) from CDCl₃ ($\delta_{\text{H}} = 7.26$ ppm, $\delta_{\text{C}} = 77.16$ ppm), CD₃OD ($\delta_{\text{H}} = 3.31$ ppm, $\delta_{\text{C}} = 49.00$ ppm). J values are expressed in Hz. Mass spectra were obtained with a Finnigan LCQ Advantage MAX (ion trap) apparatus equipped with an electrospray source. High-resolution mass spectra were obtained with a Varian MAT 311 spectrometer using electrospray analysis. Analytical HPLC was performed on a Thermo Electron Surveyor instrument equipped with a PDA detector under the following conditions: Thermo Hypersil GOLD C18 column (5 μm , 4.6 x 100 mm) with CH₃CN and 0.1% aq. trifluoroacetic acid (TFA) as eluents [0.1% aq. TFA/ CH₃CN (90/10) (5 min), followed by a linear 10% to 100% CH₃CN gradient (45 min)] at a flow rate of 1.0 mL/min and with UV detection Max Plot 220–360 nm. The syntheses of alcohols **1** and **2** have been reported previously.^[13]

Methyl 3-(benzyloxy)-6-(5-(piperidin-1-yl)pent-1-yn-1-yl)picolinate (3). To a mixture of alcohol **1** (200 mg, 0.62 mmol) in dry CH₂Cl₂ (6 mL), Et₃N (259 μL , 1.8 mmol, 3 equiv.) and methanesulfonyl chloride (71 μL , 0.9 mmol, 1.5 equiv.) were added. The mixture was refluxed for 4 h. The resulting solution was cooled to rt, filtrated under celite and concentrated under reduced pressure. To a solution of the crude product in CH₃CN (7 mL), piperidine (51 mg, 0.62 mmol, 1 equiv.) and K₂CO₃ (250 mg, 1.8 mmol, 3 equiv.) were successively added. The solution was heated under reflux for 16 h and then cooled at rt. Salts were removed by filtration. Concentration under reduced pressure and purification by flash chromatography (cyclohexane/EtOAc 2/8 to 100%, v/v) provided the desired product **3** as an orange oil (104 mg, 44%). *Rf* = 0.3 (cyclohexane/EtOAc 2/8, v/v). ¹H NMR (300 MHz, CDCl₃): $\delta = 1.41$ – 1.45 (m, 2H), 1.60 – 1.68 (m, 4H), 1.79 – 1.90 (m, 2H), 2.39 (t, *J* = 6.9 Hz, 2H), 2.56 – 2.61 (m, 6H), 3.86 (s, 3H), 5.11 (s, 2H), 7.20 – 7.36 (m, 7H). ¹³C NMR (75 MHz, CDCl₃): $\delta = 17.3$, 23.5 , 24.3 , 24.6 , 52.6 , 54.0 , 57.5 , 70.8 , 79.9 , 89.0 , 121.8 , 126.9 , 128.2 , 128.7 , 130.1 , 135.1 , 135.4 , 140.0 , 152.9 , 164.8 . MS (ESI+): *m/z* (%): 393 (100) [M+H]⁺.

Methyl 3-hydroxy-6-(4-(piperidin-1-yl)butyl)picolinate (7). To a solution of compound **3** (60 mg, 0.16 mmol) in a degassed mixture of MeOH/EtOAc (7/3.5 mL), Pearlman's catalyst (45 mg, 0.03 mmol, 0.2 equiv., 20% Pd, moisture 50%) was added. The solution was bubbled with H₂ and the reaction was stirred at rt under H₂ atmosphere (1 atm) for 1 h. The mixture was filtrated through celite[®] and concentrated under reduced pressure to furnish the desired product **7** as a yellow solid (36 mg, 77%). ¹H NMR (300 MHz, CDCl₃): $\delta = 1.48$ – 1.59 (m, 2H), 1.66 – 1.89 (m, 8H), 2.73 – 2.86 (m, 8H), 3.97 (s, 3H), 7.24 (s, 2H). ¹³C NMR (75 MHz, CDCl₃): $\delta = 22.6$, 23.2 , 23.7 , 27.3 , 36.7 , 53.2 , 53.4 , 57.6 , 126.9 , 128.9 , 129.4 , 152.9 , 157.3 , 170.0 . MS (ESI+): *m/z* (%): 293 (100) [M+H]⁺.

3-Hydroxy-6-(5-(piperidin-1-yl)pentyl)picolinaldehyde (11). To a solution of compound **7** (60 mg, 0.2 mmol) in dry CH₂Cl₂ (2 mL), lutidine (67 μL , 0.6 mmol, 3 equiv.) and TBDMSOTf (135 μL , 0.6 mmol, 3 equiv.) were successively added. The mixture was stirred at rt for 5 h under argon atmosphere. The mixture was washed with NaCl sat., dried over MgSO₄, and concentrated under reduced pressure. To a solution of the resulting residue in dry CH₂Cl₂ (2 mL), dropwise DIBAL-H (490 μL , 1M in CH₂Cl₂, 0.5 mmol, 2.5 equiv.) was added at -78°C. Then, the reaction mixture was stirred at this temperature for 12 min. The reaction was quenched with MeOH (490 μL) and the mixture was allowed to warm at room temperature. The organic layer was washed with an aqueous solution of NaOH (1 M), dried over MgSO₄ and concentrated under reduced pressure. TBAF (215 μL , 1M in THF, 0.21 mmol, 1.1 equiv.) was added at 0 °C to the residue in dry THF (10 mL), and the mixture was stirred for 16 h at this temperature. After concentration under reduced pressure, chromatography on silica gel (EtOAc/MeOH 9/1 + 1% solution of NH₃ 30%, v/v/v) afforded the desired compound **11** as a brown oil (24

mg, 44%). *Rf* = 0.3 (EtOAc/MeOH 9/1 + 1% solution of NH₃ 30%, v/v/v). ¹H NMR (300 MHz, CDCl₃): $\delta = 1.32$ – 1.51 (m, 4H), 1.58 – 1.80 (m, 8H), 2.40 – 2.45 (m, 2H), 2.48 – 2.52 (m, 4H), 2.78 (t, *J* = 7.8 Hz, 2H), 7.27 – 7.32 (m, 2H), 10.02 (s, 1H). ¹³C NMR (75 MHz, CDCl₃): $\delta = 24.0$, 25.3 , 26.1 , 27.2 , 29.6 , 37.3 , 54.5 , 59.1 , 126.5 , 129.9 , 135.8 , 154.9 , 157.1 , 198.9 . MS (ESI+): *m/z* (%): 277 (100) [M+H]⁺.

3-Hydroxy-6-(5-(piperidin-1-yl)pentyl)picolinaldehyde oxime (15). To a solution of aldehyde **11** (24 mg, 0.087 mmol) in dry EtOH (1 mL), NH₂OH.HCl (7.3 mg, 0.1 mmol, 1.2 equiv.) and NaOAc (9.2 mg, 0.11 mmol, 1.3 equiv.) were successively added. The mixture was stirred at rt for 1 h under an argon atmosphere. Concentration under reduced pressure and purification by silica gel chromatography (EtOAc/MeOH 8/2 + 1% solution of NH₃ 30%, v/v/v) afforded the desired oxime **15** as a white solid (11 mg, 43%). *Rf* = 0.1 (EtOAc/MeOH 9/1 + 1% solution of NH₃ 30%, v/v/v). ¹H NMR (300 MHz, CD₃OD): $\delta = 1.28$ – 1.42 (m, 2H), 1.57 – 1.63 (m, 2H), 1.58 – 1.77 (m, 8H), 2.69 – 2.76 (m, 4H), 2.81 – 2.87 (m, 4H), 7.18 (d, *J* = 8.4 Hz, 1H), 7.26 (d, *J* = 8.4 Hz, 1H), 8.28 (s, 1H). ¹³C NMR (75 MHz, CD₃OD): $\delta = 23.8$, 25.3 , 25.9 , 27.7 , 30.8 , 37.6 , 54.8 , 59.2 , 125.4 , 126.2 , 136.4 , 152.8 , 154.3 . MS (ESI+): *m/z* (%): 292 (100) [M+H]⁺. HRMS (ESI+): *m/z* calcd for C₁₆H₂₆N₃O₂ 292.2025; found: 292.2023. HPLC: *t_R* = 7.48 min, purity = 99.8%.

Methyl 3-(benzyloxy)-6-(4-morpholinobut-1-yn-1-yl)picolinate (4). To a mixture of alcohol **2** (200 mg, 0.64 mmol) in dry CH₂Cl₂ (7 mL), Et₃N (267 μL , 1.9 mmol, 3 equiv.) and methanesulfonyl chloride (74 μL , 0.95 mmol, 1.5 equiv.) were added. The mixture was refluxed for 4 h. The resulting solution was cooled to rt, filtrated under celite[®] and concentrated under reduced pressure. To a solution of the crude product in CH₃CN (6 mL), morpholine (56 μL , 0.64 mmol) and K₂CO₃ (266 mg, 2 mmol, 3 equiv.) were added. The solution was heated under reflux for 14 h and then cooled at rt. Salts were removed by filtration. Concentration under reduced pressure and purification by flash chromatography (cyclohexane/EtOAc 9/1 + 1% solution of NH₃ 30%, v/v/v) gave the desired product **4** as a yellow oil (80 mg, 32%). *Rf* = 0.2 (cyclohexane/EtOAc 8/2 + 1% solution of NH₃ 30%, v/v/v). ¹H NMR (300 MHz, CDCl₃): $\delta = 2.49$ – 2.52 (m, 4H), 2.57 – 2.69 (m, 4H), 3.71 – 3.74 (m, 4H), 3.96 (s, 3H), 5.20 (s, 2H), 7.27 – 7.46 (m, 7H). ¹³C NMR (75 MHz, CDCl₃): $\delta = 17.4$, 52.6 , 53.3 , 57.1 , 66.8 , 67.0 , 70.8 , 80.0 , 88.2 , 121.8 , 126.9 , 128.2 , 128.7 , 129.9 , 135.2 , 135.5 , 140.1 , 152.9 , 164.8 . MS (ESI+): *m/z* (%): 381 (100) [M+H]⁺.

Methyl 3-hydroxy-6-(4-morpholinobutyl)picolinate (8). To a solution of **4** (80 mg, 0.2 mmol) in a degassed mixture of MeOH/EtOAc (8/4 mL), Pearlman's catalyst (58 mg, 0.04 mmol, 0.2 equiv., 20% Pd, moisture 50%) was added. The solution was bubbled with H₂ and the reaction was stirred at rt under H₂ atmosphere (1 atm) for 1 h. The mixture was filtrated through celite and concentrated under reduced pressure to furnish the desired product **8** as a yellow solid (55 mg, 89%). ¹H NMR (300 MHz, CDCl₃): $\delta = 1.68$ (t, *J* = 6.9 Hz, 4H), 2.56 – 2.61 (m, 2H), 2.68 – 2.79 (m, 6H), 3.83 (t, *J* = 4.5 Hz, 4H), 3.96 (s, 3H), 7.23 (s, 2H). ¹³C NMR (75 MHz, CDCl₃): $\delta = 24.3$, 27.3 , 36.8 , 52.7 , 53.1 , 58.1 , 65.2 , 126.8 , 128.8 , 129.2 , 153.1 , 157.2 , 170.0 . MS (ESI+): *m/z* (%): 295 (100) [M+H]⁺.

3-Hydroxy-6-(4-morpholinobutyl)picolinaldehyde (12). To a solution of methyl ester **8** (55 mg, 0.18 mmol) in dry CH₂Cl₂ (2 mL), 2,6-lutidine (63 μL , 0.54 mmol, 3 equiv.) and TBDMSOTf (63 μL , 0.54 mmol, 3 equiv.) were successively added. The mixture was stirred at rt for 3.5 h under argon atmosphere. It was then washed with a saturated aqueous solution of NaCl, dried over MgSO₄, and concentrated under reduced pressure. To a solution of the resulting residue in dry CH₂Cl₂ (2 mL), DIBAL-H (450 μL , 1 M in CH₂Cl₂, 0.45 mmol, 2.5 equiv.) was added dropwise at -78°C. Then, the reaction mixture was stirred at this temperature for 12 min. The reaction was quenched with MeOH (450 μL), and the mixture was allowed to warm at room temperature. The organic layer was washed with an aqueous solution of NaOH (1 M), dried over

MgSO₄, and concentrated under reduced pressure. TBAF (200 μL, 1M in THF, 0.20 mmol, 1.1 equiv.) was added at 0 °C to the residue in dry THF (2 mL), and the mixture was stirred overnight at this temperature. After concentration under reduced pressure, chromatography on silica gel (CH₂Cl₂/MeOH 95/5, v/v) afforded access to the desired product **12** as a yellow solid (12 mg, 24%). *R_f* = 0.1 (CH₂Cl₂/MeOH 96/4, v/v). ¹H NMR (300 MHz, CDCl₃): δ = 1.56–1.61 (m, 2H), 1.70–1.80 (m, 2H), 2.39 (t, *J* = 7.5 Hz, 2H), 2.44 (t, *J* = 4.5 Hz, 4H), 2.79 (t, *J* = 7.5 Hz, 2H), 3.71 (t, *J* = 4.5 Hz, 4H), 7.25–7.31 (m, 2H), 10.01 (s, 1H). ¹³C NMR (75 MHz, CDCl₃): δ = 26.1, 27.6, 37.2, 53.8, 58.9, 66.9, 126.5, 129.8, 135.8, 154.7, 157.1, 198.8. MS (ESI+): *m/z* (%): 265 (100) [M+H]⁺.

3-Hydroxy-6-(4-morpholinobutyl)picolinaldehyde oxime (16). To a solution of aldehyde **12** (12 mg, 0.043 mmol) in dry EtOH (1 mL), NH₂OH.HCl (3.6 mg, 0.052 mmol, 1.2 equiv.) and NaOAc (4.6 mg, 0.056 mmol, 1.3 equiv.) were successively added. The mixture was stirred at rt for 1 h under an argon atmosphere. After concentration under reduced pressure, chromatography on a silica gel (CH₂Cl₂/MeOH 92/8 to 90/10, v/v) afforded access to oxime **16** as a yellow solid (10.8 mg, 86%). *R_f* = 0.3 (CH₂Cl₂/MeOH 90/10, v/v). ¹H NMR (300 MHz, CD₃OD): δ = 1.53–1.63 (m, 2H), 1.67–1.75 (m, 2H), 2.50 (t, *J* = 6 Hz, 2H), 2.57 (t, *J* = 4.5 Hz, 4H), 2.75 (t, *J* = 7.2 Hz, 2H), 3.71 (t, *J* = 4.5 Hz, 4H), 7.19 (d, *J* = 8.7 Hz, 1H), 7.25 (d, *J* = 8.6 Hz, 1H), 8.28 (s, 1H). ¹³C NMR (75 MHz, CD₃OD): δ = 26.3, 28.8, 54.5, 59.6, 67.2, 125.4, 126.0, 136.3, 152.8, 153.8, 154.3. MS (ESI+): *m/z* (%): 280 (100) [M+H]⁺. HRMS (ESI+): *m/z* calcd for C₁₄H₂₁N₃O₃ 280.1620; found: 280.1624. HPLC: *t_R* = 14.8 min, purity = 98.1%.

Methyl 3-(benzyloxy)-6-(5-morpholinopent-1-yn-1-yl)picolinate (5). To a mixture of alcohol **1** (400 mg, 1.23 mmol) in dry CH₂Cl₂ (10 mL), Et₃N (520 μL, 3.7 mmol, 3 equiv.) and methanesulfonyl chloride (143 μL, 1.9 mmol, 1.5 equiv.) were added. The mixture was refluxed for 4 h. The resulting solution was cooled to rt, filtrated under celite and concentrated under reduced pressure. To a solution of the crude product in CH₃CN (12 mL), morpholine (106 μL, 1.23 mmol, 1 equiv.) and K₂CO₃ (511 mg, 3.7 mmol, 3 equiv.) were added. The solution was heated under reflux for 16 h and then cooled at rt. Salts were removed by filtration. Concentration under reduced pressure and purification by flash chromatography (CH₂Cl₂/MeOH 98/2 to 97/3, v/v) afforded the desired product **5** as a yellow oil (350 mg, 72%). *R_f* = 0.1 (CH₂Cl₂/MeOH 98/2, v/v). ¹H NMR (300 MHz, CDCl₃): δ = 1.77 (q, *J* = 6.9 Hz, 2H), 2.41–2.48 (m, 8H), 3.67–3.71 (m, 4H), 3.93 (s, 3H, H₇), 5.16 (s, 2H), 7.28–7.44 (m, 7H). ¹³C NMR (75 MHz, CDCl₃): δ = 16.8, 24.9, 52.2, 53.2, 57.3, 66.5, 70.3, 79.2, 89.5, 121.4, 126.5, 127.7, 128.2, 129.6, 134.9, 135.2, 139.7, 152.4, 164.4. MS (ESI+): *m/z* (%): 395 (100) [M+H]⁺.

Methyl 3-hydroxy-6-(5-morpholinopentyl)picolinate (9). To a solution of **5** (350 mg, 0.89 mmol) in a degassed mixture of MeOH/EtOAc (50 mL, v/v: 2/1), Pearlman's catalyst (254 mg, 0.18 mmol, 0.2 equiv., 20% Pd, moisture 50%) was added. The solution was bubbled with H₂, and the reaction was stirred at rt under H₂ atmosphere (1 atm) for 2.5 h. The mixture was filtrated through celite and concentrated under reduced pressure to furnish the desired product **9** as a yellow solid (190 mg, 66%). *R_f* = 0.1 (CH₂Cl₂/MeOH 98/2 + 1% solution of NH₃ 30%, v/v/v). ¹H NMR (300 MHz, CDCl₃): δ = 1.21–1.32 (m, 2H), 1.39–1.47 (m, 2H), 1.54–1.64 (m, 2H), 2.22 (t, *J* = 7.5 Hz, 2H), 2.33–2.33 (m, 4H), 2.67 (t, *J* = 8.1 Hz, 2H), 3.57–3.60 (m, 4H), 3.91 (s, 3H), 7.17 (s, 2H). ¹³C NMR (75 MHz, CDCl₃): δ = 26.1, 27.0, 29.8, 37.4, 53.0, 53.6, 58.8, 66.7, 126.5, 128.6, 129.0, 153.8, 157.0, 170.0. MS (ESI+): *m/z* (%): 309 (100) [M+H]⁺.

3-Hydroxy-6-(5-morpholinopentyl)picolinaldehyde (13). To a solution of compound **9** (1.6 g, 5.2 mmol) in dry CH₂Cl₂ (70 mL), lutidine (1.5 mL, 15.8 mmol, 3 equiv.) and TBDMSOTf (4.6 mL, 15.8 mmol, 3 equiv.) were successively added. The mixture was stirred at rt overnight under argon atmosphere. The mixture was washed with NaCl sat., dried over MgSO₄, and concentrated under reduced pressure. To a solution of the resulting

residue in dry CH₂Cl₂ (100 mL), DIBAL-H (13 mL, 1M in CH₂Cl₂, 13 mmol, 2.5 equiv.) was added dropwise at -78 °C. Then, the reaction mixture was stirred at this temperature for 15 min. The reaction was quenched with MeOH (13 mL), and the mixture was allowed to warm at room temperature. The organic layer was washed with an aqueous solution of NaOH (1 M), dried over MgSO₄, and concentrated under reduced pressure. Then, TBAF (5.7 mL, 1M in THF, 5.7 mmol, 1.1 equiv.) was added at 0 °C to the residue in dry THF (65 mL) and the mixture was stirred overnight at this temperature. After concentration under reduced pressure, chromatography on silica gel (DCM/MeOH 99/1 to 95/5, v/v) afforded the desired compound **13** as a yellow oil (573 mg, 40%). *R_f* = 0.1 (DCM/MeOH 95/5, v/v). ¹H NMR (300 MHz, CDCl₃) δ 10.06 (s, 1H), 7.33 (d, *J* = 1.6 Hz, 2H), 3.73 (m, 4H), 2.82 (dd, *J* = 10.3, 5.2 Hz, 2H), 2.52–2.42 (m, 4H), 2.42–2.30 (m, 2H), 1.88–1.69 (m, 2H), 1.69–1.51 (m, 2H), 1.51–1.35 (m, 2H). ¹³C NMR (75 MHz, CDCl₃) δ 199.1, 157.3, 155.3, 136.1, 130.1, 126.7, 77.2, 67.3, 59.4, 54.1, 37.6, 29.9, 27.5, 26.7. MS (ESI+): *m/z* (%): 279 (100) [M+H]⁺. HRMS (ESI+): *m/z* calcd for C₁₅H₂₃N₂O₃ 279.1709; found: 279.1707.

3-Hydroxy-6-(5-morpholinopentyl)picolinaldehyde oxime (17). To a solution of aldehyde **13** (573 mg, 2.06 mmol) in dry MeOH (50 mL), NH₂OH.HCl (170 mg, 2.43 mmol, 1.2 equiv.) and NaOAc (217 mg, 2.62 mmol, 1.3 equiv.) were successively added. The mixture was stirred at rt for 1 h under argon atmosphere. Concentration under reduced pressure and purification by silica gel chromatography (DCM/MeOH 99/1 to 94/6, v/v) afforded the desired oxime **17** as a white solid (461 mg, 76%). *R_f* = 0.7 (EtOAc/MeOH 8/2, v/v). ¹H NMR (300 MHz, MeOD) δ 8.15 (s, 1H), 7.11 (d, *J* = 8.5 Hz, 1H), 6.99 (d, *J* = 8.5 Hz, 1H), 3.66–3.40 (m, 4H), 2.71–2.47 (m, 2H), 2.31 (s, 4H), 2.25–2.08 (m, 2H), 1.67–1.48 (m, 2H), 1.40 (m, 2H), 1.21 (m, 2H). ¹³C NMR (75 MHz, MeOD) δ 154.6, 153.8, 152.9, 136.2, 126.0, 125.3, 67.5, 60.0, 54.7, 37.8, 31.1, 28.1, 26.9. MS (ESI+): *m/z* (%): 294 (100) [M+H]⁺. HRMS (ESI+): *m/z* calcd for C₁₅H₂₄N₃O₃ 294.1818; found: 294.1821. HPLC: *t_R* = 15.5 min, purity = 97.9%.

Methyl 3-(benzyloxy)-6-(5-(6,7-dimethoxy-3,4-dihydroisoquinolin-2(1H)-yl) pent-1-ynyl) picolinate (6). Methanesulfonyl chloride (58 μL, 1.5 equiv.) was added dropwise to a solution of alcohol **1** (162 mg, 0.5 mmol) and triethylamine (210 μL, 3 equiv) in dry CH₂Cl₂ (5 mL). The solution was heated under reflux for 4 h, and then concentrated under reduced pressure. To a solution of the crude product in dry CH₃CN (20 mL), 6,7-dimethoxy-1,2,3,4-tetrahydroisoquinoline hydrochloride (190 mg, 1 equiv.) and K₂CO₃ (261 g, 4 equiv.) were added. The mixture was refluxed for 48 h. The crude mixture was filtered, concentrated under reduced pressure, and purified by flash chromatography on silica gel (EtOAc/MeOH, 95:5, v/v) to give **6** (146 mg, 62%) as a colorless oil. *R_f* = 0.1. ¹H NMR (300 MHz, CDCl₃) δ (ppm) 1.93 (qt, *J* = 6.9 Hz, 2H), 2.51 (t, *J* = 6.9 Hz, 2H), 2.63 (t, *J* = 6.9 Hz, 2H), 2.72 (t, *J* = 5.4 Hz, 2H), 2.83 (t, *J* = 5.4 Hz, 2H), 3.57 (s, 2H), 3.83 (s, 3H), 3.84 (s, 3H), 3.96 (s, 3H), 5.19 (s, 2H), 6.53 (s, 1H), 6.60 (s, 1H), 7.25–7.45 (m, 7H). ¹³C NMR (75 MHz, CDCl₃) δ (ppm) 17.4, 26.0, 28.7, 51.0, 52.7, 55.7, 55.8, 55.9, 57.2, 70.7, 79.5, 90.1, 109.4, 112.3, 121.7, 126.2, 126.6, 126.9, 128.2, 128.7, 130.0, 135.4, 135.5, 139.9, 147.1, 147.4, 152.9, 164.8.

6-(5-(6,7-Dimethoxy-3,4-dihydroisoquinolin-2(1H)-yl)pentyl)-3-hydroxypicolinaldehyde (14). To a solution of **6** (110 mg, 0.22 mmol) in degassed MeOH (20 mL), Pearlman's catalyst (63 mg, 0.2 equiv., 20% Pd, moisture 50%) was added. The solution was bubbled with H₂ and the reaction was stirred at rt under H₂ atmosphere (1 atm) for 15 h. The mixture was filtrated through celite and concentrated under reduced pressure to give the crude **10**. To a solution of the residue in dry DMF (3 mL), imidazole (45 mg, 3 equiv.) and TBDMSCl (72 mg, 2.2 equiv.) were successively added. The mixture was stirred at rt for 2 h under an argon atmosphere. The organic layer was washed with brine (5 times), dried over MgSO₄, and concentrated under reduced pressure. To a solution of the resulting residue in dry CH₂Cl₂ (10 mL), DIBAL-H (0.44 mL, 1 M in

CH₂Cl₂, 2 equiv.) was added dropwise at -78 °C. Then, the reaction mixture was stirred at this temperature for 10 min. The reaction was quenched with MeOH (0.44 mL) and the mixture was allowed to warm at rt. The organic layer was washed with an aqueous NaOH (1 M), dried over MgSO₄, and concentrated under reduced pressure. Then, TBAF (240 µL, 1.1 equiv., 1 M in THF) was added at 0 °C to the residue in dry THF (20 mL), and the mixture was stirred for 30 min at this temperature. After concentration under reduced pressure, purification by flash chromatography on silica gel (EtOAc/MeOH 8:2, v/v) afforded **14** (9.0 mg, 11%) as a pale-yellow oil. *R*_f = 0.2. ¹H NMR (300 MHz, CDCl₃) δ (ppm) 1.33–1.43 (m, 2H), 1.52–1.73 (m, 4H), 2.50–2.58 (m, 2H), 2.69–2.79 (m, 6H), 3.60 (s, 2H), 3.76 (s, 3H), 3.78 (s, 3H), 3.97 (br s, 1H), 6.45 (s, 1H), 6.52 (s, 1H), 7.18–7.25 (m, 2H), 9.96 (s, 1H), 10.60 (br s, 1H). ¹³C NMR (75 MHz, CDCl₃) δ (ppm) 26.5, 27.1, 29.6, 37.2, 50.4, 55.8, 55.9, 57.3, 109.3, 111.2, 125.5, 126.4, 129.8, 135.7, 138.5, 147.4, 147.7, 154.9, 157.0, 198.8. MS (ESI+) *m/z* (%): 385 (100) [M+H]⁺.

6-(5-(6,7-Dimethoxy-3,4-dihydroisoquinolin-2(1H-yl)pentyl)-3-hydroxypicolinaldehyde oxime (18). To a solution of **14** (13 mg, 28 µmol) in absolute EtOH (1 mL), HONH₂HCl (2.9 mg, 1.5 equiv.) and NaOAc (3.5 mg, 1.5 equiv.) were added successively. The mixture was stirred at rt for 30 min under argon atmosphere. After concentration under reduced pressure, the residue was purified by flash chromatography on silica gel (cyclohexane/EtOAc 1:1) to give oxime **18** (10 mg, 76%) as a white solid. *R*_f = 0.45 (cyclohexane/EtOAc 1:1). ¹H NMR (300 MHz, CDCl₃) δ (ppm) 1.33–1.43 (m, 2H), 1.55–1.73 (m, 4H), 2.55–2.72 (m, 2H), 2.85–2.96 (m, 4H), 3.74 (s, 1H), 3.81 (s, 3H), 3.82 (s, 3H), 6.51 (s, 1H), 6.58 (s, 1H), 6.95 (d, *J* = 8.4 Hz, 2H), 7.10 (d, *J* = 8.4 Hz, 2H), 8.28 (s, 1H), 9.88 (br s, 1H). ¹³C NMR (75 MHz, CDCl₃) δ (ppm) 14.2, 22.7, 26.1, 26.9, 37.1, 50.3, 54.7, 55.8, 55.9, 57.3, 76.6, 109.3, 111.2, 123.8, 124.3, 125.1, 135.1, 147.5, 147.8, 152.4, 153.7, 160.6, 171.9. MS (ESI+) *m/z* (%): 476 (100) [M+H]⁺. HRMS (ESI+): *m/z* calcd for C₂₂H₃₀N₃O₄ 400.2236; found: 400.2230. HPLC: *t*_R = 16.0 min (purity = 96%).

Methyl 3-(benzyloxy)-6-(4-morpholinobut-1-yn-1-yl)picolinate (4). To a mixture of alcohol **2** (200 mg, 0.64 mmol) in dry CH₂Cl₂ (7 mL), Et₃N (267 µL, 1.9 mmol, 3 equiv.) and *methanesulfonyl chloride* (74 µL, 0.95 mmol, 1.5 equiv.) were added. The mixture was refluxed for 4 h. The resulting solution was cooled to rt, filtrated under celite and concentrated under reduced pressure. To a solution of the crude product in CH₃CN (6 mL), morpholine (56 µL, 0.64 mmol) and K₂CO₃ (266 mg, 2 mmol, 3 equiv.) were added. The solution was heated under reflux for 14 h, and then cooled at rt. Salts were removed by filtration. Concentration under reduced pressure and purification by flash chromatography (cyclohexane/EtOAc 9/1 + 1% solution of NH₃ 30%, v/v/v) gave the desired product **4** as a yellow oil (80 mg, 32%). *R*_f = 0.2 (cyclohexane/EtOAc 8/2 + 1% solution of NH₃ 30%, v/v/v). ¹H NMR (300 MHz, CDCl₃): δ = 2.49–2.52 (m, 4H), 2.57–2.69 (m, 4H), 3.71–3.74 (m, 4H), 3.96 (s, 3H), 5.20 (s, 2H), 7.27–7.46 (m, 7H). ¹³C NMR (75 MHz, CDCl₃): δ = 17.4, 52.6, 53.3, 57.1, 66.8, 67.0, 70.8, 80.0, 88.2, 121.8, 126.9, 128.2, 128.7, 129.9, 135.2, 135.5, 140.1, 152.9, 164.8. MS (ESI+): *m/z* (%): 381 (100) [M+H]⁺.

Methyl 3-hydroxy-6-(4-morpholinobutyl)picolinate (8). To a solution of **4** (80 mg, 0.2 mmol) in a degassed mixture of MeOH/EtOAc (8/4 mL), Pearlman's catalyst (58 mg, 0.04 mmol, 0.2 equiv., 20% Pd, moisture 50%) was added. The solution was bubbled with H₂ and the reaction was stirred at rt under H₂ atmosphere (1 atm) for 1 h. The mixture was filtrated through celite and concentrated under reduced pressure to furnish the desired product **8** as a yellow solid (55 mg, 89%). ¹H NMR (300 MHz, CDCl₃): δ = 1.68 (t, *J* = 6.9 Hz, 4H), 2.56–2.61 (m, 2H), 2.68–2.79 (m, 6H), 3.83 (t, *J* = 4.5 Hz, 4H), 3.96 (s, 3H), 7.23 (s, 2H). ¹³C NMR (75 MHz, CDCl₃): δ = 24.3, 27.3, 36.8, 52.7, 53.1, 58.1, 65.2, 126.8, 128.8, 129.2, 153.1, 157.2, 170.0. MS (ESI+): *m/z* (%): 295 (100) [M+H]⁺.

3-Hydroxy-6-(4-morpholinobutyl)picolinaldehyde (12). To a solution of methyl ester **8** (55 mg, 0.18 mmol) in dry CH₂Cl₂ (2 mL), 2,6-lutidine (63 µL, 0.54 mmol, 3 equiv.) and TBDMSOTf (63 µL, 0.54 mmol, 3 equiv.) were successively added. The mixture was stirred at rt for 3.5 h under argon atmosphere. The mixture was washed with a saturated aqueous solution of NaCl, dried over MgSO₄, and concentrated under reduced pressure. To a solution of the resulting residue in dry CH₂Cl₂ (2 mL), DIBAL-H (450 µL, 1 M in CH₂Cl₂, 0.45 mmol, 2.5 equiv.) was added dropwise at -78 °C. Then, the reaction mixture was stirred at this temperature for 12 min. The reaction was quenched with MeOH (450 µL), and the mixture was allowed to warm at room temperature. The organic layer was washed with an aqueous solution of NaOH (1 M), dried over MgSO₄ and concentrated under reduced pressure. Then, TBAF (200 µL, 1 M in THF, 0.20 mmol, 1.1 equiv.) was added at 0 °C to the residue in dry THF (2 mL), and the mixture was stirred overnight at this temperature. After concentration under reduced pressure, chromatography on silica gel (CH₂Cl₂/MeOH 95/5, v/v) afforded access to the desired product **12** as a yellow solid (12 mg, 24%). *R*_f = 0.1 (CH₂Cl₂/MeOH 96/4, v/v). ¹H NMR (300 MHz, CDCl₃): δ = 1.56–1.61 (m, 2H), 1.70–1.80 (m, 2H), 2.39 (t, *J* = 7.5 Hz, 2H), 2.44 (t, *J* = 4.5 Hz, 4H), 2.79 (t, *J* = 7.5 Hz, 2H), 3.71 (t, *J* = 4.5 Hz, 4H), 7.25–7.31 (m, 2H), 10.01 (s, 1H). ¹³C NMR (75 MHz, CDCl₃): δ = 26.1, 27.6, 37.2, 53.8, 58.9, 66.9, 126.5, 129.8, 135.8, 154.7, 157.1, 198.8. MS (ESI+): *m/z* (%): 265 (100) [M+H]⁺.

3-Hydroxy-6-(4-morpholinobutyl)picolinaldehyde oxime (16). To a solution of aldehyde **12** (12 mg, 0.043 mmol) in dry EtOH (1 mL), NH₂OH.HCl (3.6 mg, 0.052 mmol, 1.2 equiv.) and NaOAc (4.6 mg, 0.056 mmol, 1.3 equiv.) were successively added. The mixture was stirred at rt for 1 h under argon atmosphere. After concentration under reduced pressure, chromatography on silica gel (CH₂Cl₂/MeOH 92/8 to 90/10, v/v) afforded access to oxime **16** as a yellow solid (10.8 mg, 86%). *R*_f = 0.3 (CH₂Cl₂/MeOH 90/10, v/v). ¹H NMR (300 MHz, CD₃OD): δ = 1.53–1.63 (m, 2H), 1.67–1.75 (m, 2H), 2.50 (t, *J* = 6 Hz, 2H), 2.57 (t, *J* = 4.5 Hz, 4H), 2.75 (t, *J* = 7.2 Hz, 2H), 3.71 (t, *J* = 4.5 Hz, 4H), 7.19 (d, *J* = 8.7 Hz, 1H), 7.25 (d, *J* = 8.6 Hz, 1H), 8.28 (s, 1H). ¹³C NMR (75 MHz, CD₃OD): δ = 26.3, 28.8, 54.5, 59.6, 67.2, 125.4, 126.0, 136.3, 152.8, 153.8, 154.3. MS (ESI+): *m/z* (%): 280 (100) [M+H]⁺. HRMS (ESI+): *m/z* calcd for C₁₄H₂₁N₃O₃ 280.1620; found: 280.1624. HPLC: *t*_R = 14.8 min, purity = 98.1%.

Reversible inhibition and reactivation measurements. A stock solution of oximes was prepared in dimethyl sulfoxide (DMSO; Kemika, Zagreb, Croatia), methanol (Kemika, Zagreb, Croatia) or water. Further dilutions were prepared in water or 0.1 M sodium phosphate pH 7.4. HI-6 dichloride monohydrate was a gift from Dr. Kamil Kuča and Dr. Daniel Jun (Faculty of Military Health Sciences, University of Defence, Hradec Kralove, Czech Republic). Tabun, VX, sarin and cyclosarin were purchased from NC Laboratory (Spiez, Switzerland), while paraoxon-ethyl was purchased from Sigma-Aldrich (St. Louis, MO, USA). OP stock solutions (5000 µg/mL) were made in isopropyl alcohol, and further dilutions were made in water just before use, except for paraoxon-ethyl whose stock (2750 µg/mL) and further dilutions were prepared in ethanol. Acetylthiocholine iodide (ATCh), 5,5'-dithiobis(2-nitrobenzoic acid) (DTNB), and bovine serum albumin (BSA) were purchased from Sigma-Aldrich (St. Louis, MO, USA).

Reversible inhibition of enzymes by oximes was measured in the presence of ATCh (0.05–1.0 mM) in order to determine the enzyme-oxime dissociation constant (*K*_i). The oxime was added to the mixture containing the enzyme and DTNB (final 0.3 mM), and upon addition of the ATCh, enzyme activity was measured. The activity was corrected for non-enzymatic substrate degradation by an oxime (oximolysis), and DMSO was kept below 0.15% to attenuate its inhibitory effect on AChE activity. The *K*_i was evaluated from the experimental data according to the Hunter-Downs equation and the procedure described previously.^[20b]

For reactivation experiments, the enzyme was incubated with a 10-fold excess of the OP for 30-60 min, achieving 90–100% inhibition. The incubation mixture was filtrated using a filtration column Strata® C18-E tubes (Phenomenex, Torrance, CA, USA) to remove the excess of unconjugated OP. The inhibited enzyme was then added to the reactivation mixture containing the oxime in 0.01% BSA/0.1 M sodium phosphate buffer pH 7.4 to initiate reactivation. At a designated time point, an aliquot was diluted in phosphate buffer containing DTNB, and upon addition of ATCh, enzyme activity was measured. The final concentrations of ATCh and DTNB were 1.0 and 0.3 mM, respectively. An equivalent sample of an uninhibited enzyme was passed through a parallel column, diluted to the same extent as the reactivation mixture, and control activity was measured in the presence of an oxime at the same concentrations used for reactivation. Both the activities of the control and the reactivation mixture were corrected for oximolysis. No significant spontaneous reactivation of the phosphorylated enzyme occurred.

One oxime concentration (0.2 mM; or 0.1 mM for **19**) or a wide range of oxime concentrations were used to determine the first-order reactivation rate constant at a given oxime concentration (k_{obs}), maximal percentage of reactivation ($\text{React}_{\text{max}}$) and kinetic constants (maximal first-order reactivation rate constant k_{+2} , overall second-order reactivation rate constant k and phosphorylated enzyme-oxime dissociation constant K_{ox}) as described previously.^[18b]

Reversible inhibition and reactivation measurements were performed at 25 °C using the Ellman spectrophotometric method^[40] at 412 nm on a Tecan Infinite M200PRO microplate reader (Tecan Austria GmbH, Salzburg, Austria) or a CARY 300 spectrophotometer (Varian Inc., Mulgrave, Australia), respectively.

Ex vivo scavenging assay. *Ex vivo* degradation of OPs with oximes **16** and **18** was performed in whole human blood (hWB) incubated with 10-fold and 50-fold concentrations (0.7 μM and 3.4 μM , respectively) of VX, sarin, cyclosarin and paraoxon relative to the concentration of the AChE in hWB, which accounts for 80% of total blood cholinesterase activity (20% BChE). After 1 h of incubation (achieving 95–100% inhibition), oxime (1.0 mM) was added to the mixture. At specified time intervals, an aliquot was taken for enzyme activity measurements and results were expressed as percentage reactivation, as described previously.^[16c] Enzyme activity measurements were performed as described for the reactivation assay at 436 nm on a CARY 300 spectrophotometer (Varian Inc., Mulgrave, Australia) at 25 °C. hWB was collected from a healthy female donor at the Institute for Medical Research and Occupational Health, Zagreb, Croatia following approval by the Ethics Committee of the Institute.

Crystallization and structure determination. *Torpedo californica* AChE (TcAChE) was purified as described previously.^[41] Trigonal crystals were obtained in hanging drops with the vapor diffusion method by mixing an equal volume of protein solution (13 mg/mL) and precipitant solution (28–36% PEG 200, MES 100 mM pH 5.4) at 21 °C. Before carrying out soaking experiments, the DMSO solvent was evaporated from oxime **17**. To achieve evaporation, 2 μL of reactivator solutions (at 2-20 mM) in 100 % DMSO were added onto the surface of crystallization supports from EasyXtal crystallization trays (Qiagen) and stored in a fume hood during 24 h. After complete DMSO evaporation, 2 μL of the precipitant solution were added and pipetted exhaustively to dissolve the maximum amount of reactivator remaining on the surface of the crystallization supports. TcAChE crystals were then transferred into the resulting drop and incubated during 24 h before flash-cooling in liquid nitrogen. Data collection was performed at 100 K on BM30A-FIP beamline at the European Synchrotron Radiation Facility, with $\lambda = 0.98 \text{ \AA}$ and an ADSC Q315r CCD detector. Diffraction patterns were indexed, integrated and scaled using XDS and XSCALE^[42]. Phase determination was performed

by molecular replacement in Phaser,^[43] and refinement was carried out with Phenix^[44]. Reactivator's geometry descriptions and restraints were obtained from Avogadro^[45] and Phenix.elbow^[46], respectively. Real space refinement and model analysis were performed using Coot.^[47] Coordinates and structure factors were deposited in the PDB with the assigned code 6EWK. For data collection and refinement statistics see **Table S1**.

Molecular modelling of oxime complexes with phosphorylated AChE and BChE. The crystal structures of VX-inhibited mouse AChE (PDB: 2Y2U)^[26] and human BChE (PDB: 2PM8)^[48] were used for molecular docking using Biovia Discovery Studio Client v17.2 (Accelrys, San Diego, CA, USA). The model of the cyclosarin-hBChE conjugate was prepared by superposition of the crystal structures of hBChE and cyclosarin-inhibited mouse AChE (PDB:3ZLU),⁴² and translation of cyclosarin moiety to the BChE Ser198O γ . The structural model of the cyclosarin-hBChE conjugate with an alternate conformation of the cyclosarin moiety was obtained by a 90° rotation of the cyclohexyl ring.

Oxime structures were created and minimized using the MMFF94 force field implemented in ChemBio3D Ultra 12.0 (PerkinElmer, Inc., Waltham, MA, USA). The Dock Ligands protocol (CDOCKER) was used to generate 30 top-scored docking poses of each oxime in the defined active site of the enzyme ($r = 13 \text{ \AA}$) sorted by CHARMM energy (interaction energy plus ligand strain), where a more negative value corresponds to more favourable binding. Depending on the orientations of specific functional groups, two or three generated poses were selected for minimization (Minimization protocol with Smart Minimizer algorithm, as implemented in Biovia Discovery Studio Client v17.2, Accelrys, San Diego, CA, USA) and intermolecular bond analyses (i.e., electrostatic, hydrophobic, and H-bonds).

The alignment of amino acid sequences of hAChE, mAChE, and TcAChE was done using AlignSequences protocol from Biovia Discovery Studio Client v17.2 (Accelrys, San Diego, CA, USA).

pKa determination. The absorption spectra of oximes were scanned at 220-450 nm at 0.1 M phosphate pH 6.0-11.3 on a CARY 300 spectrophotometer (Varian Inc., Mulgrave, Australia) at 25 °C. Dissociation constants, K_{a} , were determined from the absorption maximums as described previously using the equation^[30]:

$$A_{\text{tot}} = \frac{A_1 \times [H^+]^2 + A_2 \times [H^+] \times K_{a1} + A_3 \times K_{a1} \times K_{a2}}{[H^+]^2 + [H^+] \times K_{a1} + K_{a1} \times K_{a2}} \quad (1)$$

where A_{tot} is the sum of the absorption fractions of all ionization species, while A_1 , A_2 and A_3 are values of absorbance that correspond to different ionization species. The hydrogen ion concentration is represented by $[H^+]$. The acid-base equilibrium between the various species is defined by dissociation constants K_{a1} and K_{a2} , and was determined using Prism6 software (Graph Pad Software, San Diego, CA, USA).^[16d, 30]

Calculation of molecular properties and in silico prediction of BBB penetration. The physicochemical properties of the oximes such as the logarithm of the octanol-water partition coefficient (logP), pH-dependent lipophilicity coefficient (logD), polar surface area ($\text{PSA}/\text{\AA}^2$), number of H-bond donors (HBD) and acceptors (HBA), number of rotatable bonds (RB), pK_{a} values, and microspecies at a specific pH, were determined using Marvin software (version 16.11.7.0, ChemAxon, Budapest, Hungary) at an ionic strength of $c(\text{Na}^+, \text{K}^+) = 0.1 \text{ M}$ and $c(\text{Cl}^-) = 0.1 \text{ M}$ and 25 °C. The obtained results were compared to the recommendations for physicochemical properties of a successful central nervous system drug^[33] or used in an algorithm for calculating the CNS MPO score (Central Nervous System Multi-Parameter Optimization) that defines the probability of a compound being a CNS-active drug.^[34b]

Permeability test (PAMPA-BBB). A parallel artificial membrane permeation assay for the BBB was used, following the method described

by Di *et al.*^[35] The *in vitro* permeability (P_e) of fourteen commercial drugs through a lipid extract of the porcine brain membrane together with the test compounds was determined. Commercial drugs and assayed compounds were tested using a mixture of PBS:EtOH (70:30). Assay validation was performed by comparing the experimental permeability with reported values of the commercial drugs, and linear correlation between the experimental and reported permeability of the fourteen commercial drugs using the parallel artificial membrane permeation assay was evaluated ($y = 1.5758x - 1.1459$; $R^2 = 0.9241$). From this equation, and taking into account the limits for BBB permeation reported by Di *et al.*, the ranges of permeability were established as follows: compounds with high BBB permeation (CNS+): P_e (10^{-6} cm s^{-1}) > 5.157 ; compounds with low BBB permeation (CNS-): P_e (10^{-6} cm s^{-1}) < 2.006 , and compounds with uncertain BBB permeation (CNS+/-): $5.157 > P_e$ (10^{-6} cm s^{-1}) > 2.006 .

Acknowledgements

This work was supported by the *Direction Générale de l'Armement* (through a PhD Fellowship to A.B.), the *Agence Nationale de la Recherche* (ANR) (project ReCNS-AChE, grant number ANR-13-ASTR-0002-02), the program PHC COGITO (2015–2016) (33068WE), the interministerial program of R&D against CBRNE risks and the Croatian Science Foundation (project CHOLINESTERASE, grant number IP-11-2013-4307). This work was partially supported by INSA Rouen, Rouen-Normandie University, Centre *National de la Recherche Scientifique* (CNRS), *Région Haute-Normandie* (CRUNCH network), and the Labex SynOrg (ANR-11-LABX-0029).

Keywords: acetylcholinesterase • butyrylcholinesterase • oxime • nerve agents • CNS

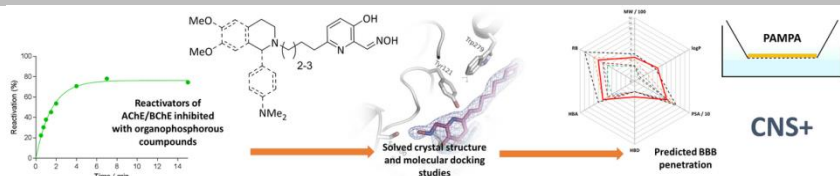
Supporting Information. Content: **S1.** Reactivation of OP-phosphorylated hAChE with oximes; **S2.** Crystal structure of the complex of TcAChE and oxime **17**; **S3.** Sequence alignment between mouse, human, and *Torpedo californica* AChE; **S4.** Docking of oximes into TcAChE, VX-mAChE and cyclosarin-hBChE; **S5.** *In vitro* determination of pK_a values. This material is available free of charge via the Internet at <http://...>

- [1] a) M. Eddleston, N. A. Buckley, P. Eyer and A. H. Dawson, *Lancet* **2008**, *371*, 597-607; b) M. Eddleston, L. Karalliedde, N. Buckley, R. Fernando, G. Hutchinson, G. Isbister, F. Konradsen, D. Murray, J. C. Piola, N. Senanayake, R. Sheriff, S. Singh and S. B. Siwach, *Lancet* **2002**, *360*, 1163-1167.
- [2] a) E. Dolgin, *Nat. Med.* **2013**, *19*, 1194-1195; b) A. T. Tu, *Toxin Rev.* **2007**, *26*, 231-274.
- [3] P. Taylor in *Anticholinesterase agents*, Eds.: A. G. Hardman, J. G. Limbird and L. E. Gilman, McGraw-Hill, New York, **1995**, pp. 161-176.
- [4] a) J. H. McDonough, Jr. and T. M. Shih, *Neurosci. Biobehav. Rev.* **1997**, *21*, 559-579; b) T. Okumura, K. Taki, K. Suzuki, T. Yoshida, Y. Kuroiwa and T. Satoh in *Chapter 4 - The Tokyo subway sarin attack: Acute and delayed health effects in survivors*, (Ed. R. C. Gupta), Academic Press, Boston, **2015**, pp. 27-35.
- [5] a) B. Li, J. A. Stribley, A. Ticu, W. Xie, L. M. Schopfer, P. Hammond, S. Brimijoin, S. H. Hinrichs and O. Lockridge, *J. Neurochem.* **2000**, *75*, 1320-1331; b) J. Minic, A. Chatonnet, E. Krejci and J. Molgo, *Br. J. Pharmacol.* **2003**, *138*, 177-187; c) K. A. Petrov, E. Girard, A. D. Nikitashina, C. Colasante, V. Bernard, L. Nurullin, J. Leroy, D. Samigullin, O. Colak, E. Nikolsky, B. Plaud and E. Krejci, *J. Neurosci.* **2014**, *34*, 11870-11883.
- [6] M. P. Stojiljković and M. Jokanović, *Arh. Hig. Rada. Toksikol.* **2006**, *57*, 435-443.
- [7] a) Z. Kovarik, M. Čalić, G. Šinko, A. Bosak, S. Berend, A. Lucić Vrdoljak and B. Radić, *Chem. Biol. Interact.* **2008**, *175*, 173-179; b) Z. Kovarik, Z. Radić, H. A. Berman, V. Simeon-Rudolf, E. Reiner and P. Taylor, *Biochemistry* **2004**, *43*, 3222-3229; c) F. Worek and H. Thiermann, *Pharmacol. Ther.* **2013**, *139*, 249-259.
- [8] a) Z. Radic, N. A. Pickering, D. C. Vellom, S. Camp and P. Taylor, *Biochemistry* **1993**, *32*, 12074-12084; b) P. Taylor and Z. Radic, *Annu. Rev. Pharmacol. Toxicol.* **1994**, *34*, 281-320; c) Y. Nicolet, O. Lockridge, P. Masson, J. C. Fontecilla-Camps and F. Nachon, *J. Biol. Chem.* **2003**, *278*, 41141-41147.
- [9] W. N. Aldridge and E. Reiner, *Enzyme Inhibitors as Substrates. Interactions of Esterases with Esters of Organophosphorus and Carbamic Acids (Frontiers of Biology, Vol. 26)*, Elsevier, **1972**, p. 328 pp.
- [10] G. Mercey, T. Verdelet, J. Renou, M. Kliachyna, R. Baati, F. Nachon, L. Jean and P.-Y. Renard, *Acc. Chem. Res.* **2012**, *45*, 756-766.
- [11] D. E. Lorke, H. Kalasz, G. A. Petroianu and K. Tekes, *Curr. Med. Chem.* **2008**, *15*, 743-753.
- [12] M. Katalinić, N. Maček Hrvat, J. Žďárová Karasová, J. Misik and Z. Kovarik, *Arh. Hig. Rada. Toksikol.* **2015**, *66*, 291-298.
- [13] a) M. C. de Koning, M. van Grol and D. Noort, *Toxicol. Lett.* **2011**, *206*, 54-59; b) J. Kalisiak, E. C. Ralph and J. R. Cashman, *J. Med. Chem.* **2012**, *55*, 465-474; c) J. Kalisiak, E. C. Ralph, J. Zhang and J. R. Cashman, *J. Med. Chem.* **2011**, *54*, 3319-3330; d) Z. Kovarik, N. Maček, R. K. Sit, Z. Radić, V. V. Fokin, K. B. Sharpless and P. Taylor, *Chem. Biol. Interact.* **2013**, *203*, 77-80; e) N. Maraković, A. Knežević, V. Vinković, Z. Kovarik and G. Šinko, *Chem. Biol. Interact.* **2016**, *259*, 122-132; f) G. Mercey, J. Renou, T. Verdelet, M. Kliachyna, R. Baati, E. Gillon, M. Arboléas, M. Loidice, F. Nachon, L. Jean and P.-Y. Renard, *J. Med. Chem.* **2012**, *55*, 10791-10795; g) G. Mercey, T. Verdelet, G. Saint-André, E. Gillon, A. Wagner, R. Baati, L. Jean, F. Nachon and P.-Y. Renard, *Chem. Commun.* **2011**, *47*, 5295-5297; h) Z. Radić, R. K. Sit, E. Garcia, L. Zhang, S. Berend, Z. Kovarik, G. Amitai, V. V. Fokin, K. Barry Sharpless and P. Taylor, *Chem. Biol. Interact.* **2013**, *203*, 67-71; i) J. Renou, J. Dias, G. Mercey, T. Verdelet, C. Rousseau, A.-J. Gastellier, M. Arboleas, M. Touvrety-Loidice, R. Baati, L. Jean, F. Nachon and P.-Y. Renard, *RSC Advances* **2016**, *6*, 17929-17940; j) J. Renou, M. Loidice, M. Arboleas, R. Baati, L. Jean, F. Nachon and P.-Y. Renard, *Chem. Commun.* **2014**, *50*, 3947-3950; k) J. Renou, G. Mercey, T. Verdelet, E. Păunescu, E. Gillon, M. Arboléas, M. Loidice, M. Kliachyna, R. Baati, F. Nachon, L. Jean and P.-Y. Renard, *Chem. Biol. Interact.* **2013**, *203*, 81-84; l) R. K. Sit, V. V. Fokin, G. Amitai, K. B. Sharpless, P. Taylor and Z. Radić, *J. Med. Chem.* **2014**, *57*, 1378-1389; m) R. K. Sit, Z. Radić, V. Gerardi, L. Zhang, E. Garcia, M. Katalinić, G. Amitai, Z. Kovarik, V. V. Fokin, K. B. Sharpless and P. Taylor, *J. Biol. Chem.* **2011**, *286*, 19422-19430; n) Z. Radić, R. K. Sit, Z. Kovarik, S. Berend, E. Garcia, L. Zhang, G. Amitai, C. Green, B. Radic, V. V. Fokin, K. B. Sharpless and P. Taylor, *J. Biol. Chem.* **2012**, *287*, 11798-11809; o) Z. Radić, T. Dale, Z. Kovarik, S. Berend, E. Garcia, L. Zhang, G. Amitai, C. Green, B. Radic, B. M. Duggan, D. Ajami, J. Rebek and P. Taylor, *Biochem. J* **2013**, *450*, 231-242.
- [14] M. Lobell, L. Molnár and G. M. Keserü, *J. Pharm. Sci.* **2003**, *92*, 360-370.
- [15] R. K. Sit, Z. Radic, V. Gerardi, L. Zhang, E. Garcia, M. Katalinic, G. Amitai, Z. Kovarik, V. V. Fokin, K. B. Sharpless and P. Taylor, *J. Biol. Chem.* **2011**, *286*, 19422-19430.
- [16] a) Z. Kovarik, N. Maček Hrvat, M. Katalinić, R. K. Sit, A. Paradyse, S. Žunec, K. Musilek, V. V. Fokin, P. Taylor and Z. Radić, *Chem. Res. Toxicol.* **2015**, *28*, 1036-1044; b) Z. Kovarik, Z. Radić, H. A. Berman

- and P. Taylor, *Toxicology* **2007**, 233, 79-84; c) N. Maček Hrvat, S. Žunec, P. Taylor, Z. Radić and Z. Kovarik, *Chem. Biol. Interact.* **2016**, 259, 148-153; d) Z. Radić, T. Dale, Z. Kovarik, S. Berend, E. Garcia, L. Zhang, G. Amitai, C. Green, B. Radic, B. M. Duggan, D. Ajami, J. Rebek and P. Taylor, *Biochem. J* **2013**, 450, 231-242.
- [17] A. G. Calas, J. Dias, C. Rousseau, M. Arboleas, M. Touvrey-Loiodice, G. Mercey, L. Jean, P. Y. Renard and F. Nachon, *Chem. Biol. Interact.* **2017**, 267, 11-16.
- [18] a) Z. Kovarik, N. Cibán, Z. Radić, V. Simeon-Rudolf and P. Taylor, *Biochem. Biophys. Res. Commun.* **2006**, 342, 973-978; b) Z. Kovarik, M. Čalić, A. Bosak, G. Šinko and D. Jelić, *Croat. Chem. Acta* **2008**, 81, 47-57.
- [19] P. M. Lundy, M. G. Hamilton, T. W. Sawyer and J. Mikler, *Toxicology* **2011**, 285, 90-96.
- [20] a) M. Katalinić, N. Maček Hrvat, K. Baumann, S. Morasi Piperčić, S. Makarić, S. Tomić, O. Jović, T. Hrenar, A. Miličević, D. Jelić, S. Žunec, I. Primožič and Z. Kovarik, *Toxicol. Appl. Pharmacol.* **2016**, 310, 195-204; b) M. Katalinić, A. Zandona, A. Ramić, T. Zorbaz, I. Primožič and Z. Kovarik, *Molecules* **2017**, 22.
- [21] A. Lucić Vrdoljak, M. Čalić, B. Radić, S. Berend, D. Jun, K. Kuca and Z. Kovarik, *Toxicology* **2006**, 228, 41-50.
- [22] A. Allgardsson, L. Berg, C. Akfur, A. Hornberg, F. Worek, A. Linusson and F. J. Ekstrom, *Proc. Natl. Acad. Sci. U. S. A.* **2016**, 113, 5514-5519.
- [23] C. B. Millard, G. Koellner, A. Ordentlich, A. Shafferman, I. Silman and J. L. Sussman, *J. Am. Chem. Soc.* **1999**, 121, 9883-9884.
- [24] P. M. Legler, I. Soojhawon and C. B. Millard, *Acta Crystallogr. Sect. D. Biol. Crystallogr.* **2015**, 71, 1788-1798.
- [25] a) B. Sanson, F. Nachon, J.-P. Colletier, M.-T. Froment, L. Toker, H. M. Greenblatt, J. L. Sussman, Y. Ashani, P. Masson, I. Silman and M. Weik, *J. Med. Chem.* **2009**, 52, 7593-7603; b) M. C. Franklin, M. J. Rudolph, C. Ginter, M. S. Cassidy and J. Cheung, *Proteins* **2016**, 84, 1246-1256.
- [26] C. Akfur, E. Artursson and F. Ekstrom, *To be published*.
- [27] a) M. Harel, I. Schalk, L. Ehret-Sabatier, F. Bouet, M. Goeldner, C. Hirth, P. H. Axelsen, I. Silman and J. L. Sussman, *Proc. Natl. Acad. Sci. U. S. A.* **1993**, 90, 9031-9035; b) F. Nachon, E. Carletti, C. Ronco, M. Trovaslet, Y. Nicolet, L. Jean and P. Y. Renard, *Biochem. J* **2013**, 453, 393-399; c) E. H. Rydberg, B. Brumshtein, H. M. Greenblatt, D. M. Wong, D. Shaya, L. D. Williams, P. R. Carlier, Y. P. Pang, I. Silman and J. L. Sussman, *J. Med. Chem.* **2006**, 49, 5491-5500.
- [28] A. d. S. Gonçalves, T. C. C. França, J. D. Figueroa-Villar and P. G. Pascutti, *J. Braz. Chem. Soc.* **2011**, 22, 155-165.
- [29] Y. Li, L. Du, Y. Hu, X. Sun and J. Hu, *Can. J. Chem.* **2012**, 90, 376-383.
- [30] G. Šinko, M. Čalić and Z. Kovarik, *FEBS Lett.* **2006**, 580, 3167-3172.
- [31] A. E. Gillam in Eds.: E. S. Stern and C. J. Timmons), Edward Arnold, London, **1970**, p. 149.
- [32] D. S. Bohle, Z. Chua, I. Perepichka and K. Rosadiuk, *Chem. Eur. J.* **2013**, 19, 4223-4229.
- [33] H. Pajouhesh and G. R. Lenz, *NeuroRx* **2005**, 2, 541-553.
- [34] a) T. T. Wager, R. Y. Chandrasekaran, X. Hou, M. D. Troutman, P. R. Verhoest, A. Villalobos and Y. Will, *ACS Chem. Neurosci.* **2010**, 1, 420-434; b) T. T. Wager, X. Hou, P. R. Verhoest and A. Villalobos, *ACS Chem. Neurosci.* **2010**, 1, 435-449; c) T. T. Wager, X. Hou, P. R. Verhoest and A. Villalobos, *ACS Chem. Neurosci.* **2016**, 7, 767-775.
- [35] L. Di, E. H. Kerns, K. Fan, O. J. McConnell and G. T. Carter, *Eur. J. Med. Chem.* **2003**, 38, 223-232.
- [36] B. J. Bennion, N. A. Be, M. W. McNerney, V. Lao, E. M. Carlson, C. A. Valdez, M. A. Malfatti, H. A. Enright, T. H. Nguyen, F. C. Lightstone and T. S. Carpenter, *J. Phys. Chem. B* **2017**, 121, 5228-5237.
- [37] a) N. J. Abbott, A. A. Patabendige, D. E. Dolman, S. R. Yusof and D. J. Begley, *Neurobiol. Dis.* **2010**, 37, 13-25; b) A. M. Palmer and M. S. Alavijeh, *Curr. Protoc. Pharmacol.* **2013**, 62, Unit 7.15.
- [38] a) G. Cassel, L. Karlsson, L. Waara, K. W. Ang and A. Goransson-Nyberg, *Eur. J. Pharmacol.* **1997**, 332, 43-52; b) H. Kalasz, S. M. Nurulain, G. Veress, S. Antus, F. Darvas, E. Adeghate, A. Adem, F. Hashemi and K. Tekes, *J. Appl. Toxicol.* **2015**, 35, 116-123.
- [39] O. Soukup, J. Korabecny, D. Malinak, E. Nepovimova, N. L. Pham, K. Musilek, M. Hrabínova, V. Hepnarova, R. Dolezal, P. Pavek, P. Jost, T. Kobrlova, J. Jankockova, L. Gorecki, M. Psotka, T. D. Nguyen, K. Box, B. Outhwaite, M. Ceckova, A. Sofr, D. Jun and K. Kuca, *Med. Chem.* **2018**.
- [40] G. L. Ellman, K. D. Courtney, V. Andres, Jr. and R. M. Feather-Stone, *Biochem. Pharmacol.* **1961**, 7, 88-95.
- [41] J. L. Sussman, M. Harel, F. Frolow, L. Varon, L. Toker, A. H. Futerman and I. Silman, *J. Mol. Biol.* **1988**, 203, 821-823.
- [42] W. Kabsch, *Acta Crystallogr. Sect. D. Biol. Crystallogr.* **2010**, 66, 133-144.
- [43] A. J. McCoy, R. W. Grosse-Kunstleve, P. D. Adams, M. D. Winn, L. C. Storoni and R. J. Read, *J. Appl. Crystallogr.* **2007**, 40, 658-674.
- [44] P. D. Adams, P. V. Afonine, G. Bunkóczi, V. B. Chen, I. W. Davis, N. Echols, J. J. Headd, L. W. Hung, G. J. Kapral, R. W. Grosse-Kunstleve, A. J. McCoy, N. W. Moriarty, R. Oeffner, R. J. Read, D. C. Richardson, J. S. Richardson, T. C. Terwilliger and P. H. Zwart, *Acta Crystallogr. Sect. D. Biol. Crystallogr.* **2010**, 66, 213-221.
- [45] M. D. Hanwell, D. E. Curtis, D. C. Lonie, T. Vandermeersch, E. Zurek and G. R. Hutchison, *J. Cheminform.* **2012**, 4, 17.
- [46] N. W. Moriarty, R. W. Grosse-Kunstleve and P. D. Adams, *Acta Crystallogr. Sect. D. Biol. Crystallogr.* **2009**, 65, 1074-1080.
- [47] P. Emsley, B. Lohkamp, W. G. Scott and K. Cowtan, *Acta Crystallogr. Sect. D. Biol. Crystallogr.* **2010**, 66, 486-501.
- [48] M. N. Ngamela, K. Homma, O. Lockridge and O. A. Asojo, *Acta Crystallogr. Sect. F Struct. Biol. Cryst. Commun.* **2007**, 63, 723-727.
- ...

Entry for the Table of Contents

FULL PAPER



A new class of uncharged oximes tested as reactivators of human acetylcholinesterase and butyrylcholinesterase inhibited with nerve agents were more efficient than oximes in use. The crystal structure displayed a productive conformation for reactivation of both phosphorylated enzymes. Furthermore, oximes are predicted to efficiently cross the blood-brain-barrier and they could, therefore, potentially achieve significant concentrations both at the neuromuscular junction and in the brain. This, in turn, could result in an overall improved therapeutic outcome after nerve agents poisoning.

Tamara Zorbaz, Anissa Braiki, Nikola Maraković, Julien Renou, Eugenio de la Mora, Nikolina Maček Hrvat, Maja Katalinić, Israel Silman, Joel L. Sussman, Guillaume Mercey, Catherine Gomez, Romain Mougeot, Belén Pérez, Rachid Baati, Florian Nachon, Martin Weik, Ludovic Jean,* Zrinka Kovarik,* and Pierre-Yves Renard*

Potent 3-hydroxy-2-pyridine aldoxime reactivators of organophosphate-inhibited cholinesterases with predicted blood-brain barrier penetration